°Master of ScienceProposal

ASSESSING RECOVERY OF MILD TRAUMATIC BRAIN INJURY PATIENTS USING DIFFUSION TENSOR IMAGING

A Thesis

Presented to

the Faculty of the Department of Engineering Technology

University of Houston

In Partial Fulfillment

of the Requirements for the Degree

Master of Science

By

Esther Mvula

November 2016

ASSESSING RECOVERY OF MILD TRAUMATIC BRAIN INJURY PATIENTS USING DIFFUSION TENSOR IMAGING

Esther Mvula

APPROVED:

George Zouridakis, Ph.D. , Professor and Director
Dept. of Engineering Technology

Luca Pollonini, Ph.D. , Assistant Professor
Dept. of Engineering Technology

Keith Lancaster, Instructional Assistant Professor
Dept. of Information and Logistics Technology

Dean, College of Technology

Acknowledgements

Firstly, I would like to express my sincere gratitude to my advisor Dr. George Zouridakis for the continuous support during my research, for his patience, motivation, and immense knowledge. His guidance helped me in all the time of research and writing of this thesis. I could not have imagined having a better advisor and mentor for my Master's thesis.

Besides my advisor, I would like to thank the rest of my thesis committee: Dr. Luca Pollonini, and Prof. Keith Lancaster, for their insightful comments and encouragement, but also for the hard questions which incited me to widen my research from various perspectives.

Last but not least, I would like to thank my family for their spiritual and emotional support throughout this work and in my life in general.

ASSESSING RECOVERY OF MILD TRAUMATIC BRAIN INJURY PATIENTS USING DIFFUSION TENSOR IMAGING

An Abstract of a Thesis

Presented to

the Faculty of the Department of Engineering Technology

University of Houston

In Partial Fulfillment

of the Requirements for the Degree

Master of Science

By

Esther Mvula

November 2016

Abstract

In this study we investigated whether Diffusion Tensor Imaging (DTI) could be used to assess recovery in patients with mild traumatic brain injury (mTBI). Thirteen acute mTBI patients 18-50 years of age and seven age- and sex-matched controls with no head injury were recruited from the emergency department of Huntington Memorial Hospital in Pasadena, CA. Images were acquired on three different visits, two weeks and four weeks, respectively, after the first recording, using a 3.0 T. Image distortions, resulting from susceptibility-induced and by eddy current-induced off-resonance fields, were corrected using routines from the software package FSL. An affine linear registration routine part of FSL was also used to align the 32 images to the reference image. For each DTI dataset, diffusion Fractional Anisotropy (FA), Mean Diffusivity (MD) or Apparent Diffusion Coefficient (ADC), and probabilistic tractography were estimated using FSL and the software package MedInria, with an FA threshold of 200, a minimum length for the detected fibers of 20 mm, and volume sampling every 5 voxels. To perform a quantitative analysis across the two groups, we first used the Johns Hopkins University tractography atlas to define 20 regions of interest (ROI), and the scans from the control subjects to create a reference database that included the mean and standard deviation values in each ROI. Then we computed z-scores for each subjects data and compared the groups using MANOVA with p value set at 0.05, corrected for multiple comparisons, considering group and visit as the independent variables.

Contents

List of Figures

List of Tables

Chapter 1

Introduction

According to the Center for Disease Control and Prevention (CDC), traumatic brain injury (TBI) is a major cause of death and disability in the United States, contributing to about 30% of all injury deaths [8]. Mild traumatic brain injury (mTBI) alone constitutes approximately 75–85% of all brain trauma cases [9]. The long-term outcome of mTBI, however, is not well characterized owing to its considerable heterogeneity. One difficulty in accurately diagnosing mild neurotrauma relates to the frequent lack of radiological evidence to support the diagnosis, which often leads clinicians to diagnose mTBI based on clinical or cognitive symptoms known to overlap with other clinical conditions[10] (e.g., hypoglycemic or vasovagal attacks and certain subtypes of mood disorders). Among the neuropsychological alterations that are commonly reported in patients with mTBI include impairment in attention, memory, psycho-motor speed, and executive functions.

1.1 Traumatic Brain Injury (TBI)

The brain is the most complex part of the human body. This three pound organ is the seat of intelligence, database of memories, interpreter of the senses, and the director of all movements. Lying in its bony shell and washed by protective fluid,the brain is also the most fragile organ in the body with the same texture and consistency as gelatin.

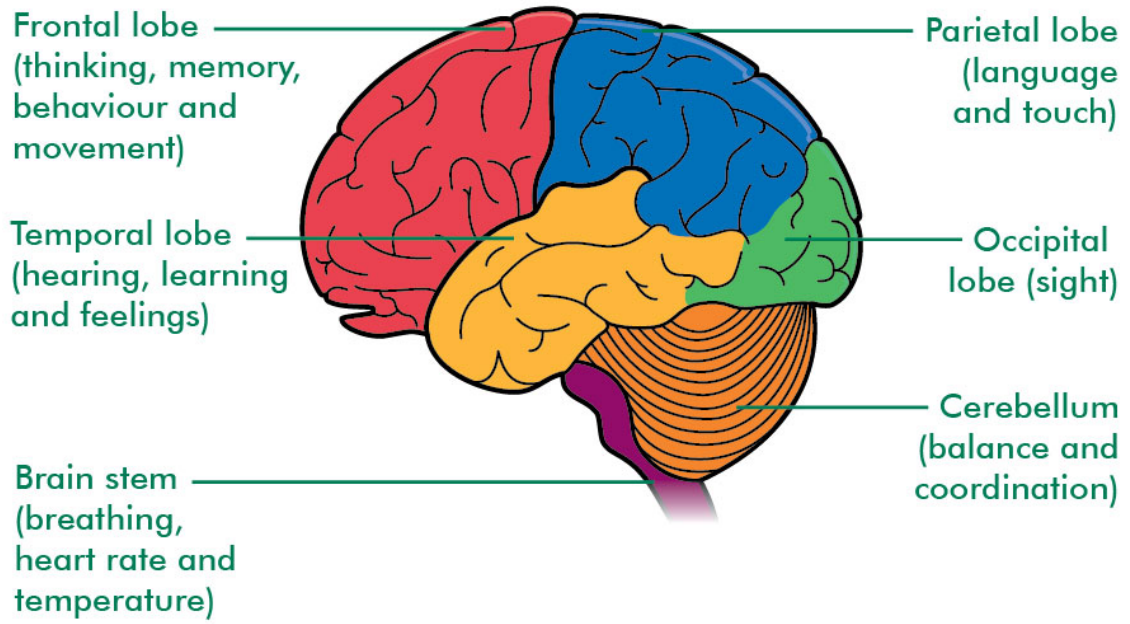

Figure 1.1: Lobes and functions of the brain[1]

Within the brain are over 100 Billions nerve cells called neurons, sending electrical and chemical signals to and from the body; each neuron has a cell body, a long nerve fiber called an axon, and projections of the cell body called dendrites.

Dendrites extend out from the cell body to receive messages from other nerve cells. Axons in the brain connect neurons with each other, which in turns provide extensive interconnections with other brain areas.

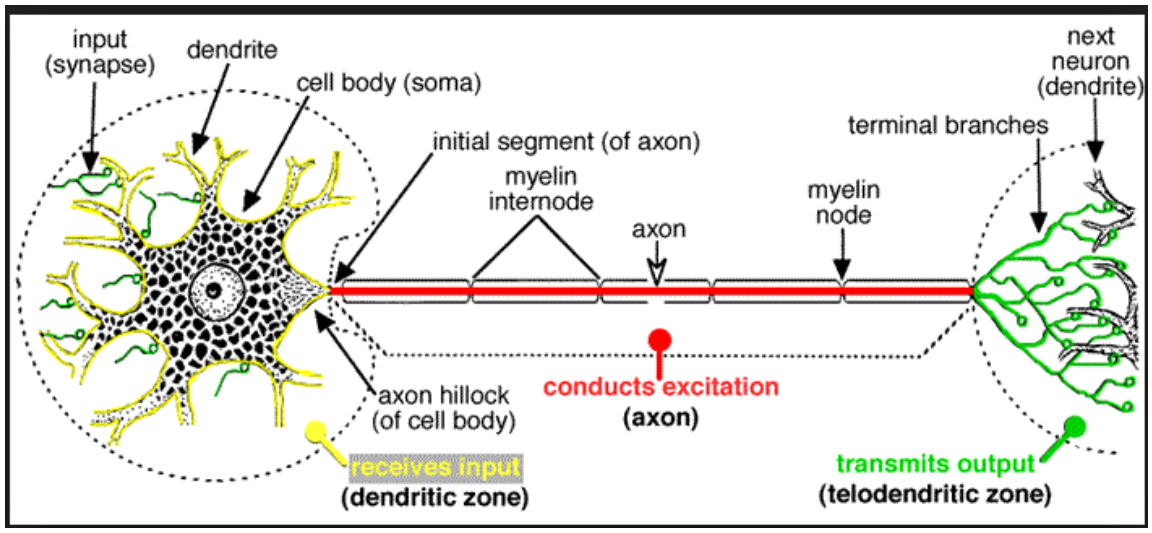

Figure 1.2: Brain Cell[2]

Because the brain and its nerve cells are so fragile, sudden rapid movement of the head can cause injuries; during one such injury called coup-contrecoup[11] or acceleration-deceleration injury[12], the brain bounces back and forth against the bony interior wall of the skull. In high speed coup-contrecoup injuries the impact may be violent enough to cause swelling and bruising of the brain tissue called a **contusion**. Howerver, in cases involving low speed coup-contrecoup injuries, the resulting damage may not be visible to the naked eye. As the brain moves back and forth within the skull, areas of varying density in the brain slide over each other at different speeds; axons crossing these junctions experience tremendous shearing forces causing them to stretch and tear from the cell body; this event is called **axonal**

shearing[13] or **Diffuse Axonal Injury(DAI)**[14].

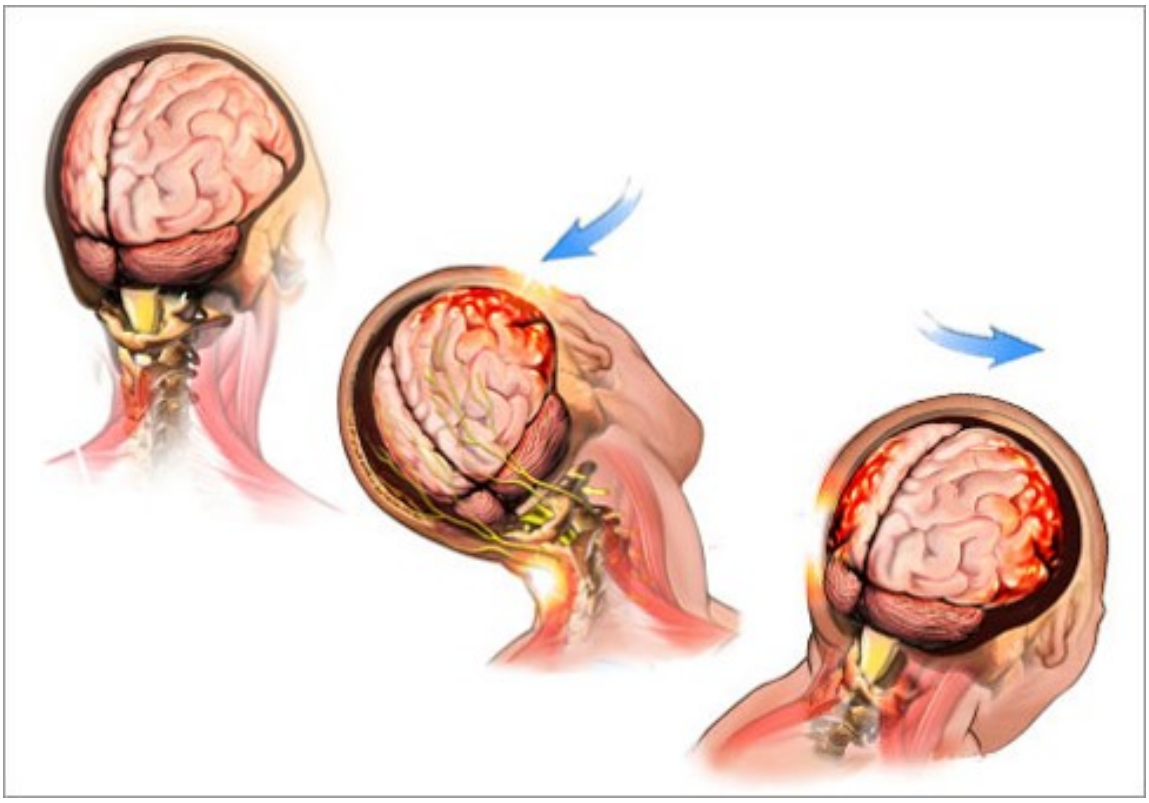

Figure 1.3: Traumatic Brain Injury[3]

Brain damage can continue to occur for hours or days after the initial injury; damage to the axon can lead to a breakdown of communication among neurons in the brain. The torn axon quickly degenerates, releasing toxic levels of chemicals called neurotransmitters into the extracellular space. In turn, many of the surrounding neurons begin to die over the next 24-48 hours, worsening the initial effect of the injury. Mild to moderate cases of DAI may result in symptoms such as brief loss of consciousness, impaired long-term memory, reduced problem-solving ability, lower social inhibition, and problems with attention and perception. Severe cases of DAI

may result in coma or persistent vegetative state. In the united states, over 1 million cases of mild traumatic brain injuries including DAI, are reported each year, and over 300,000 patients suffer long-term effects from the damage[9]. Computed Tomography (CT), and Magnetic Resonance Imaging (MRI) are test that can be performed to check for mild traumatic brain injury (mTBI); the results of these tests usually show a normal reading, and therefore doctors must rely on patient history, and a clinical exam to diagnose mTBI. Extensive research is being conducted to find methods with greater sensitivity and specificity. In 2015, Dimitriadis, Stavros I., *et al.* published **"Functional connectivity changes detected with magnetoencephalography after mild traumatic brain injury"**[15], where they analyzed brain connectivity profiles from resting state Magnetoencephalographic (MEG) recordings obtained from two groups namely mTBI patients and control subjects. Comparison of the two distinct general patterns at different frequencies using a tensor representation for the connectivity graphs and tensor subspace analysis for optimal feature extraction showed that mTBI patients could be separated from normal controls with 100% classification accuracy in the alpha band. In 2016, Antonakakis, Marios, *et al.* analyzed Cross-Frequency Coupling (CFC) profiles from resting state Magnetoencephalographic (MEG) recordings obtained from 30 mild traumatic brain injury (mTBI) patients, and their findings indicate that analysis of brain networks computed from resting-state MEG with Phase-to-Amplitude Coupling (PAC) and tensorial representation of connectivity profiles may provide a valuable biomarker for the diagnosis of mTBI and 50 controls[16]. **Diffusion Tensor Imaging** is a non-invasive method for characterizing the integrity of anatomical connections and white

matter circuitry and provides a quantitative assessment of the brain's white matter microstructure[17].

1.2 Diffusion Tensor Imaging

Both CT and ordinary MRI are like a series of still shots taken of a slice through the ear from multiple directions. The end result is a three-dimensional static picture of the anatomical structure. While this type of image gives us useful information, it is also rather limited. Diffusion Tensor Imaging (DTI) is a magnetic resonance imaging (MRI) technique which has become established in the last two decades as a valuable research tool. It is based on a modification of conventional MRI in a way that allows the non-invasive and in vivo quantification of the diffusion characteristics of water molecules[18] and [19]. To be able to understand why this DTI was used to detect mTBI, we first need to understand what diffusion is in general and what is biological diffusion in particular. Secondly we need to understand the principle behind DTI, namely Diffusion Weighed Imaging(DWI).

1.2.1 Biological Diffusion

In basic terms, diffusion is the microscopic movement of atoms and molecules in a solution or gas. In living tissues, molecules of water, salt, and other chemicals flow freely through the various tissues of our bodies. However, in certain pathological conditions such as in a tightly packed cell of tumors, or the local swelling and pressure produced by the lack of blood flow during a stroke in the brain, will create an environment that limits or restricts the movement of these various molecules. We know that diffusion is driven by the random interaction of molecules as they collide

with one another under Brownian motion. Robert Brown(21 December 1773 10 June 1858) [20]was a Scottish botanist who, in 1827 observed the continuous jittery -type motion in minor particles of starch and lipid organelles ejected from grains of pollens floating in water. It was subsequently noted that the higher the temperature of the liquid, the faster these particles moved. In his Annus Mirabilis or Miracle year of 1905, Albert Einstein published On the Movement of Small Particles Suspended in Stationary Liquids Required by the Molecular-Kinetic Theory of Heat , where he quantified Brownian motion, and established the relationship of heat, kinetic-molecular collision, and particle movement [21].In three dimensions, the Einstein diffusion equation:

$$D = \frac{\Delta r^2}{2n\Delta t} \tag{1.1}$$

States that the diffusion coefficient D(in mm^2/s) is proportional to the mean squared-displacement,(Δr^2) divided by the number of dimensions, n, and the diffusion time, Δt. The diffusion coefficient of pure water at 20°C is roughly 2.0 $\times 10^{-3} mm^2/s$ and increases at higher temperatures. In the absence of boundaries, the molecular water displacement is described by a Gaussian probability density:

$$P(\Delta r, \Delta t) = \frac{1}{\sqrt{(2\pi D\Delta t)^3}} \times \exp(\frac{-\Delta r^2}{4D\Delta t}) \tag{1.2}$$

The spread in this distribution increases with the diffusion time, Dt in Figure 1.4:

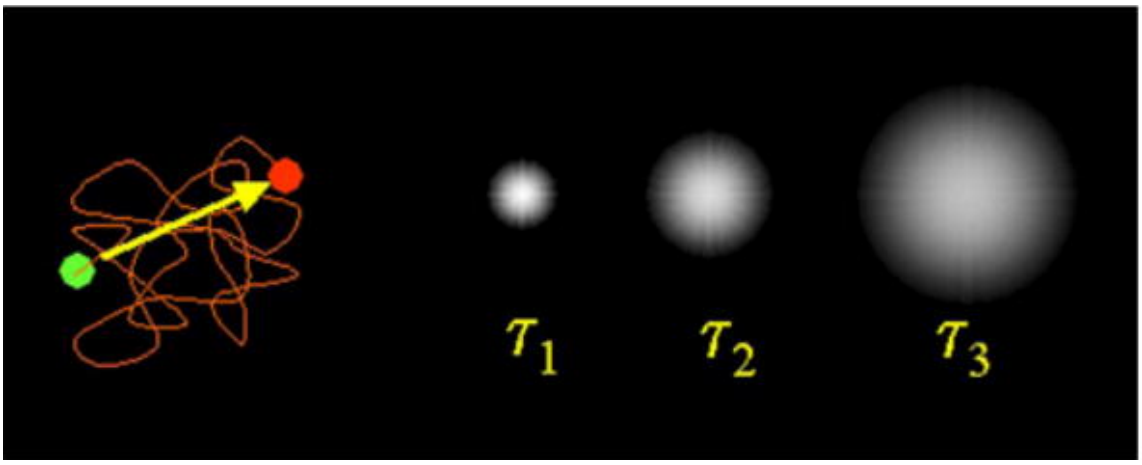

Figure 1.4: Left: Illustration of the diffusion random-walk for a single water molecule from the green location to the red location. The displacement is shown by the yellow arrow. Right three frames: Diffusion describes the displacement probability with time for a group or ensemble of water molecules. For short diffusion times (e.g., t_1), the predicted spread is compact, but increases with longer diffusion times (t_2 and t_3).[4]

In a human body, there are enumerable compartmentalized collections of fluids; for instance, the cells of our nervous system or neurons contain a cell membrane that surround a fluid environment where the organelles and nutrients required for cell life reside. The cell body of the neuron contains the cell nucleus and mitochondria. The prominent extension of the cell body, the axon, propagates the electrical impulse up and down the nerve. If we were to go deep in the cell body and observe a molecule of water, we would watch that molecule flow freely through its liquid environment as it randomly collides with other water molecules, the organelles, and various dissolved

chemicals the cell requires or produces to stay alive. Because of the rounded three dimensional configuration of the cell body, the water molecule with its two Hydrogen atoms is basically free to move in any direction. This type of unrestricted diffusion is referred to as ***Isotropic Diffusion***. Now, lets look at the axon; the long tubular configuration of the structure will restrict the movement of the diffusion of that same water molecule preferentially along the axis of the axon itself. This asymmetric movement is referred to as ***Anisotropic Diffusion***.

1.2.2 Diffusion Weighed Imaging (DWI)

Diffusion Weighted Imaging (DWI) or Diffusion-weighted Magnetic Resonance Imaging (DW-MRI) is an imaging technique that makes use of the variability of Brownian motion of water molecules in brain tissue to generate contrast in MR images[22]. To obtain diffusion-weighted images, a pair of strong gradient pulses are added to the pulse sequence. The first pulse dephases the spins, and the second pulse rephases the spins if no net movement occurs. If net movement of spins occurs between the gradient pulses, signal attenuation occurs. The degree of attenuation depends on the magnitude of molecular translation and diffusion weighting. The amount of diffusion weighting is determined by the strength of the diffusion gradients, the duration of the gradients, and the time between the gradient pulses.Diffusion imaging is performed optimally on a high-field (1.5 T) echo-planar system, but it can be accomplished with a turboSTEAM sequence on systems with conventional gradients. The diffusion data can be presented as signal intensity or as an image map of the apparent diffusion coefficient (ADC). Calculation of the ADC requires 2 or more acquisitions with different diffusion weightings. A low ADC corresponds to

high signal intensity (restricted diffusion), and a high ADC to low signal intensity on diffusion-weighted images.

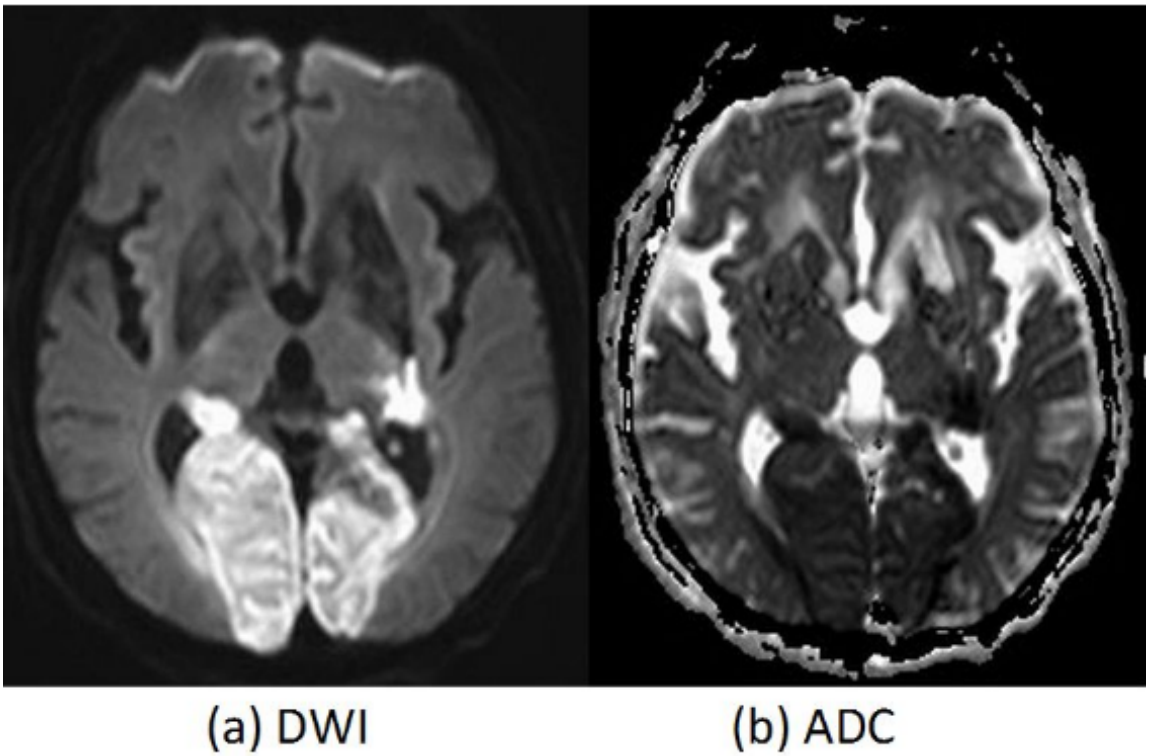

Figure 1.5: a) DWI shows hyperintense signal along bilateral posterior cerebral arterial territories. b) corresponding ADC map demonstrates hypointense signal[5]

1.2.3 Diffusion Tensor Imaging (DTI)

1.2.3.1 Introduction to DTI

The human brain is a massively interconnected organ. The entire central core of the brain known as the white matter comprises relatively large bundles of fibers that mediate communication between neurons in widely separated locations. Diffusion Tensor Imaging (DTI) is a new form of MRI that provides information about the

white matter. Researchers can trace pathways through the data provided by DTI, estimating the size and locations of white matter nerve bundles. While DWI discussed above refers to the contrast of the acquired images, DTI is a specific type of modeling of the DWI datasets. DTI principles and basic concepts have been extensively described and reviewed in the literature (Mori and Barker, 1999; Le Bihan et al., 2001; Hagmann et al., 2006; Mori and Zhang, 2006; Mori, 2007; Nucifora et al., 2007; Assaf and Pasternak, 2008; Jones, 2008, 2010b; Mukherjee et al., 2008a; Johansen-Berg and Behrens, 2009; Figueiredo et al., 2011; Thomason and Thompson, 2011; Tournier et al., 2011; Yang et al., 2011).

In summary, the basic concept behind DTI is that water molecules diffuse differently along the tissues depending on its type, integrity, architecture, and presence of barriers, giving information about its orientation and quantitative anisotropy (Chenevert et al., 1990; Moseley et al., 1990; Douek et al., 1991; Beaulieu, 2002). With DTI analysis it is possible to infer, in each voxel, properties such as the molecular diffusion rate [Mean Diffusivity (MD) or Apparent Diffusion Coefficient (ADC)], the directional preference of diffusion [Fractional Anisotropy (FA)], the axial (diffusion rate along the main axis of diffusion), and radial (rate of diffusion in the transverse direction) diffusivity. Diffusion in White Matter (WM) is less restricted along the axon and tends to be anisotropic (directionally-dependent) whereas in Gray Matter (GM) is usually less anisotropic and in the Cerebrospinal fluid (CSF) is unrestricted in all directions (isotropic) (Pierpaoli et al., 1996; Song et al., 2002; Hagmann et al., 2006). Based on this assumption, Basser and colleagues (1994a,b) modeled the diffusion process by an ellipsoid, which can mathematically be represented by a 3 3

symmetric matrix, also known as tensor (hence DTI's name origin)[23].

1.2.3.2 Applications of DTI

Because DTI is sensitive to microstructural tissue properties, it can be used in WM research and clinical work to explore WM anatomy and structure in vivo. In fact, this sensitivity, providing diffusion summary measures and tissue fiber orientation, has made DTI widely used as a clinical tool, especially in conditions where abnormalities in WM are expected (Sundgren et al., 2004; Mori and Zhang, 2006). For example, it has been successfully implemented to study patients with acute stroke or brain tumors; neurodegenerative disorders including multiple sclerosis, epilepsy, and Alzheimer's; neuropsychiatric disorders such as schizophrenia; mild cognitive impairment; developmental disorders like dyslexia, autism, and attention deficit hyperactivity disorder; movement disorders (mainly Parkinson's and Huntington's); neurogenetic developmental disorders such as Williams syndrome and fragile X syndrome; and changes in WM microstructure during neurodevelopment and in aging (Le Bihan et al., 2001; Moseley et al., 2002; Sundgren et al., 2004; Vilanova et al., 2006; Nucifora et al., 2007; Ciccarelli et al., 2008; Imfeld et al., 2009; Johansen-Berg and Behrens, 2009; Madden et al., 2009; Yamada et al., 2009; Chanraud et al., 2010; Carvalho Rangel et al., 2011; Fung et al., 2011; Hygino da Cruz Jr et al., 2011; Thomason and Thompson, 2011; Voineskos et al., 2012). DTI variables (e.g., FA, axial diffusivity) are usually related with alterations in structure (possibly due to particular conditions/disease) pointing to specific myelination levels and axonal injury (Song et al., 2002; White et al., 2008; Budde et al., 2009; Gupta et al., 2012).

1.2.3.3 DTI Measures

Once the water diffusion is measured like in equation 1.1, there are many ways we can quantify the shape of the tensors in each voxel. The commonly used measures in DTI are: Fractional Anisotropy (FA), mean diffusivity(MD) or Apparent Diffusion Coefficient (ADC), Axial Diffusivity (AD) and Radial Diffusivity (RD). In our case, we will focus on the first two values, namely FA and ADC. These values directly relate to the three main eigenvalues of the tensor, indicated in the figure below by lambda 1, lambda 2, and lambda 3.An eigenvalue of a tensor is the value of displacement or diffusion for each specific vector.

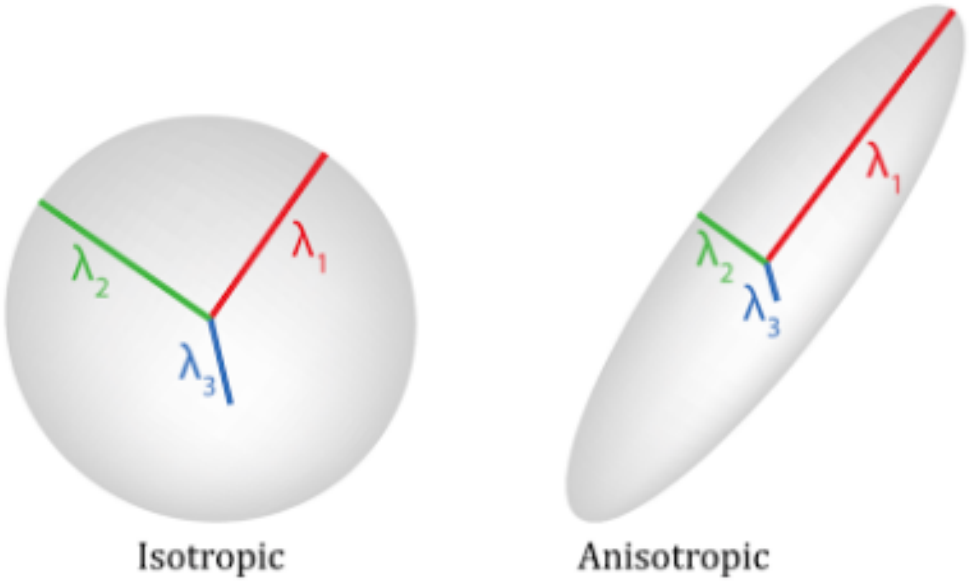

Figure 1.6: Example of Tensor Shapes [6]

As we said earlier, there are two types of diffusion: *Isotropic*, in which the tensor has roughly equal eigenvalues for each main vector, and *Anisotropic*, where the

diffusion is primarily in one direction with a main eigenvalue lambda 1.

The exact mathematical relations are shown below:

λ_1 =Axial(or Longitudinal) Diffusivity (AD)

$(\lambda_2 + \lambda_3)$ =Radial Diffusivity (RD)

$(\lambda_1 + \lambda_2 + \lambda_3)/3$ =Mean Diffusivity (MD) or Apparent Diffusion Coefficient (ADC)

$\sqrt{\frac{1}{2}} \times \frac{\sqrt{(\lambda_1-\lambda_2)^2+(\lambda_1-\lambda_3)^2+(\lambda_2-\lambda_3)^2}}{\sqrt{\lambda_1^2+\lambda_2^2+\lambda_3^2}}$ =Fractional Anisotropy (FA)

After showing all these measures and how they relate to each other, it is important to know how they relate to brain structure:

- Fractional Anisotropy: It is the summary of microstructural integrity. While FA is highly sensitive to microstructural changes, it is less specific to the type of change. In other terms, FA can measure white matter intergrity.

- Apparent Diffusion Coefficient: It is an inverse measure of the membrane density, is very similar for both GM and WM.

1.3 Objectives

The main objectif of this thesis was to investigate whether Diffusion Tensor Imaging (DTI) can be used to assess recovery in patients with mild traumatic brain injury (mTBI). First, we analyzed the two coefficients (FA and ADC) during the first visit after the trauma. Secondly, we observed if there was an improvement in these coefficients during the subsequent visits.

1.3.1 Specific Objectives

The following presents the list of specific our objectives in this study:

1. To detect mild Traumatic Brain Injury (mTBI) from patients who suffered
2. Compare our findings to the medical diagnosis
3. Assess and quantify the recovery of patients over a period of 4 to 6 weeks.

1.3.2 Achieving Specific Objectives

To achieve the specific objectives of this thesis, the following steps were taken:

- Employ two distinct groups: Patients and control subjects;
- Perform Diffusion Tensor Tractography for all the Diffusion Weighed dataset (patients and control subjects);
- Quantify the fiber tracts to detect areas of injury;
- Compare the results obtained in all the three visit to see whether the patients recovered.

This work is a part of a larger study performed at the University of Houston, Houston, TX and the Huntington Medical Research Institutes, Pasadena, CA, where the same dataset is used to find out if source connectivity analysis of resting state Magnetoencephalographic (MEG) activity can detect patients with mild traumatic brain injury (mTBI).

1.3.3 Limitations

The limitations we faced during this experiment were our sample size (Eleven patients, and seven control subjects) and the consistency of their visits. The patients and control subjects were supposed to show up for three consecutive visits, but some of them did not follow through. We know that increasing the sample size decreases the standard error according to the standard error formula:

$$\sigma_M = \frac{\sigma}{\sqrt{N}} \tag{1.3}$$

In equation 1.3, σ_M denotes the standard error, σ is the standard deviation, and N is the sample size.We can then conclude that increasing the sample size gives less variation or more precision in our results.

The rest of the thesis is divided as follows: Chapter 2 gives us a little background and related works on DTI, chapter 3 discusses the methodology of our study; the results we obtained are discussed in chapter 4 and chapter 5 gives us a brief summary and a conclusion of our work.

Chapter 2

Background

Improvements in the imaging of water diusion have been made by the development of the more complex diusion tensor imaging (DTI), which allows direct examination, in vivo, of some aspects of tissue micro-structure. DTI yields quantitative measures reecting the integrity of white-matter ber tracts, by taking advantage of the intrinsic directionality of water diusion in human brain. The diusion of water molecules is characterized by Brownian motion. When water molecules are unconstrained, the direction of motion of a given molecule is random[24]. In this chapter, we review some of the related works in both DTI technology and its clinical applications. A comprehensive literature search was conducted on AMED, Embase, MEDLINE, Ovid, PubMed, Scopus, and Web of Science for all relevant articles reporting on the use of DTI in subjects who developed PCS post-mTBI, through 20 May, 2016. The databases were searched with the following search phrase using the Boolean logic

operators OR and AND: (DTI OR diffusion tensor imaging OR diffusion tractography) AND (mTBI OR mild traumatic brain injury OR concussion) AND (post-concussive syndrome OR post-concussive syndrome OR post concussive syndrome OR postconcussion syndrome OR post-concussion syndrome OR post concussion syndrome) AND human. To ensure maximal article capture, these search terms also encompassed the following Medical Subject Headings (MeSH) terms: diffusion tensor imaging, brain injuries, and post-concussion syndrome. Manual searching of relevant journals and reference lists of studies found in the above search provided additional articles.

2.1 Mild Traumatic Brain Injury

As we said in chapter 1, mTBI constitutes approximately 75–85% of all brain trauma cases. Therefore, a lot of researches have been conducted to understand how it occurs and its symptoms, what structures of the brain are affected by it, and the methods used to detect it. In 1984, Imajo, Takeshi, and Uros Roessman studied diffuse axonal injury as a distinct form of head injury, induced by direct external forces at the lime of the trauma, and not produced by secondary changes due to a primary injury[14]. In 1993, Head, J defined a patient with mTBI as a person who has had a traumatically induced physiological disruption of the brain function, as manifested by at least one of the following: any period of loss of consciousness, any loss of memory for events immediately before of after the accident, anyalteration in mental state at the time of the accident (eg, feeling dazed, disoriented, or confused), and focal neurological deficit(s) that may or may not be transient[25]. In 2001, Gerstenbrand, F., and Ch A. Stepan named disturbance of behavior or emotional

functioning as some of the symptoms of mTBI as well as the causes[26].

2.2 Diffusion Tensor Imaging

Many studies have been performed to understand how we can use the properties of water diffusion to conduct an imaging technique that will allow us to visualize white matter tracts. The basic principles of diffusion MRI were introduced in the mid-1980s [27]; they combined Nuclear Magnetic Resonance (NMR) imaging principles with those introduced earlier to encode molecular diffusion effects in the NMR signal by using bipolar magnetic field gradient pulses[28]. Molecular diffusion refers to the random translational motion of molecules, also called Brownian motion, that results from the thermal energy carried by these molecules.

In 1976, Cleveland, G. G., *et al*[29] studied the anisotropy of the spin-diffusion coefficient Ds of water protons in skeletal muscle by pulsed NMR methods. The mid-portion of the tibialis anterior muscle of mature male rats was placed in a special sample holder by means of which the muscle fiber orientation theta relative to the diffusion direction could be varied over the range 0 degrees less than or equal to theta less than or equal to 90 degrees. These results are interpreted within the framework of a model calculation in which the diffusion equation is solved for a regular hexagonal network similar to the actin-myosin filament network. The large anisotropy, and the large reduction in the value of Ds measured parallel to the filament axes lead to two major conclusions: (a) interpretations in which the reduction in Ds is ascribed to the effect of geometrical obstructions on the diffusion of "free" water are ruled out; and, (b) there is a large fraction of the cellular water associated with the proteins in such a way that its diffusion coefficient is substantially reduced.

In 1990, Chenevert, Thomas L.,*et al*[30] performed quantitative measurements of perfusion and molecular diffusion in human white matter in two orientations of the motion-sensitization gradient to document anisotropy of these parameters. Measurements were localized to a 10 X 10-mm tissue column oriented in an anterior-to-posterior direction in the left cerebral hemisphere just above the body of the left ventricle.

In 1990, Doran, Mark, *et al.*[31] used a pulsed magnetic field gradient spin echo technique to study the brain of two volunteers and eight patients. The pulsed gradients were applied both perpendicular and parallel to the image slice. Striking changes in signal intensity were demonstrated in white matter depending on the direction in which pulsed gradients were applied.

In 1994, Basser *et al* [18] described a new NMR imaging modality, MR diffusion tensor imaging. It consisted of estimating an effective diffusion tensor, Deff, within a voxel, and then displaying useful quantities derived from it. They showed how the phenomenon of anisotropic diffusion of water (or metabolites) in anisotropic tissues, measured noninvasively by these NMR methods, was exploited to determine fiber tract orientation and mean particle displacements.

In 2004, Sundgren, P. C., *et al.* [24] reviewed the theoretical background to diffusion tensor imaging (DTI) and some of its commoner clinical applications, such as cerebral ischemia, brain maturation and traumatic brain injury. We also review its potential use in diseases such as epilepsy, multiple sclerosis, and Alzheimers disease. The value of DTI in the investigation of brain tumors and metabolic disorders was also assessed. In 2011, Jones, Derek K., and Alexander Leemans [32]

2.3 DTI and Traumatic Brain Injury

In 2005, Inglese Matilde, *et al.* [33]presented a study whose aim was to assess the presence and extent of Diffuse Axonal Injury (DAI) in patients with mild TBI. No differences in any of the histogram-derived measures were found between patients and control volunteers. Compared with controls, a significant reduction of fractional anisotropy was observed in patients' corpus callosum, internal capsule, and centrum semiovale, and there were significant increases of mean diffusivity in the corpus callosum and internal capsule. Neither histogram-derived nor regional diffusion tensor imaging metrics differed between the two groups.

In September 2007, Bazarian, Jeffrey J., *et al.* published "Diffusion tensor imaging detects clinically important axonal damage after mild traumatic brain injury: a pilot study" [34] whose goal was to detect clinically important axonal damage in cerebral white matter after mild traumatic brain injury (TBI) using diffusion tensor imaging (DTI). They evaluated a prospective, pilot study of six subjects with isolated mild TBI and six matched orthopedic controls. All subjects underwent DTI scanning, post-concussive symptom (PCS) assessment, and neurobehavioral testing within 72 h of injury. Fractional anisotropy (FA) and trace values in white matter voxels of whole brain and five preslected regions of interest (ROI) were compared in mild TBI and control subjects using a quantile approach.

In 2008, Wilde, E. A., *et al.* [35] performed diffusion tensor imaging tractography of the corpus callosum in 10 adolescents (14 to 19 years of age) with mTBI 1 to 6 days postinjury with Glasgow Coma Scale score of 15 and negative CT, and 10 age-

and gender-equivalent uninjured controls. Subjects were administered the Rivermead Post Concussion Symptoms Questionnaire and the Brief Symptom Inventory to assess self-reported cognitive, affective, and somatic symptoms.The mTBI group demonstrated increased fractional anisotropy and decreased apparent diffusion coefficient and radial diffusivity, and more intense postconcussion symptoms and emotional distress compared to the control group. Increased fractional anisotropy and decreased radial diffusivity were correlated with severity of postconcussion symptoms in the MTBI group, but not in the control group.

In 2008, Rutgers, D. R., *et al.* presented a study [36] in which the hypothesis was that patients with mild traumatic brain injury (TBI) had widespread brain white matter regions of reduced FA involving a variety of fiber bundles and showed fiber disruption on fiber tracking in a minority of these regions.Patients had on average 9.1 regions with reduced FA, with a mean region volume of 525 mm3, predominantly found in cerebral lobar white matter, cingulum, and corpus callosum. These regions mainly involved supratentorial projection fiber bundles, callosal fibers, and fronto-temporo-occipital association fiber bundles. Internal capsules and infratentorial white matter were relatively infrequently affected. Of all of the involved fiber bundles, 19.3% showed discontinuity on fiber tracking.

Chapter 3

Methods

Thirteen acute mTBI patients 18-50 years of age and seven age- and sex-matched controls with no head injury were recruited from the emergency department of Huntington Memorial Hospital in Pasadena, CA. Images were acquired on three different visits, two weeks and four weeks, respectively, after the first recording, using a 3.0 T scanner for approximately 12 min of total imaging time. Diffusion images were collected along 32 directions with an isotropic voxel size of 2.5 mm^3. An additional image with no-diffusion weighting was used as a reference. Image distortions, resulting from susceptibility-induced and by eddy current-induced off-resonance fields, were corrected using routines from the software package FSL. An affine linear registration routine part of FSL was also used to align the 32 images to the reference image. For each DTI dataset, diffusion Fractional Anisotropy (FA), Mean Diffusivity (MD), and probabilistic tractography were estimated using FSL and the software package MedInria, with an FA threshold of 200, a minimum length for the detected

fibers of 20 mm, and volume sampling every 5 voxels. To perform a quantitative analysis across the two groups, we first used the Johns Hopkins University (JHU) white-matter tractography atlas to define 20 regions of interest (ROI), and the scans from the control subjects to create a reference database that included the mean and standard deviation values in each ROI. Then we computed standard z-scores for each subjects data and compared the groups using MANOVA with p value set at 0.05, corrected for multiple comparisons, considering group and visit as the independent variables.

The following steps were taken in order to complete our study:

- Artifacts and Data Acquisition
- Quality Control and Preprocessing
- Processing and Visualization
- Quantitative Analysis: Region of Interest (ROI) Analysis

3.1 Artifacts and Data Acquisition

GE and Siemens scanners output DICOM (which stands for Digital Imaging and COmmunications in Medicine) format. While Philips scanners output PAR/REC format. While it is possible to view DICOM or PAR/REC images using specialized software, they are not suitable for processing. Formats that are more commonly used for processing and viewing is the NifTI format. NifTI stands for Neuroimaging informatics Technology Initiative, started by NIH to help streamline the available tools for neuroimaging research. To convert DICOM or PAR/REC images to NifTI

you can use software tools like dcm2nii or others[37]. The artifacts in DWI datasets are mainly related with the gradient system hardware, pulse sequence, acquisition strategy used and motion. A 3.0 T scanner was used to collect DWI data using 32 gradient directions. DWI data are generally collected to cover the entire brain by repeating the acquisition while varying the orientation or magnitude of the diffusion gradients. DWI has low Signal-to-Noise Ratio (SNR) and resolution and is very susceptible to motion (Farrell et al., 2007; Choi et al., 2011; Polders et al., 2011). To reduce the influence of motion artifacts, the scan time can be reduced. This makes the use of Single-shot Echo Planar Imaging (EPI) (Mansfield, 1977; Stehling et al., 1991; Turner et al., 1991; Nana et al., 2008) the typical strategy employed to reduce this sensitivity (Stehling et al., 1991; Turner et al., 1991; Nana et al., 2008); however, alternative sequences, such as Fast Spin Echo (FSE) (Seifert et al., 2000; Pipe et al., 2002), Line Scan Diffusion Imaging (LSDI), (Gudbjartsson et al., 1996) and Stimulated Echo Acquisition Mode (STEAM) (Nolte et al., 2000) may also be of interest to reduce artifacts (Xu et al., 2004; Mukherjee et al., 2008b; Bammer et al., 2009).

3.2 Quality Control and Preprocessing

The first step in DTI analysis is somewhat what we do in fMRI analysis, and that is we try to correct any sort of distortion or any kind of motion that went on. So, there is some analogs to DTI analysis that we see in fMRI analysis; for instance fMRI data sometimes require what we call a field map[38], and this gives us a sense of where there might have been distortions in the magnetic field, and if we have those, then we can basically take the reverse of that and try to subtract that out from the

image to get rid of that all that distortion.

Because the images acquired were in DICOM format, we had to convert them to .nii file format in order to obtain bval and bvec. The .nii file type is primarily associated with 'NIfTI-1 Data Format' by Neuroimaging Informatics Technology Initiative.

To convert our DICOM images to .nii format, we used a package tool called MRIcron[39]. The output of the conversion gave us 3 files: The compressed DWI images in one .nii.gz file, the bvec file, and the bval file.

Our bvec file contains 3 rows with 33 floating point numbers, corresponding to the number of volumes in our NITFI files. The first row contains the x elements, the second row contains the y elements and third row contains the z elements of a unit vector in the direction of the applied diffusion gradient, where the i–th elements in each row correspond together to the i–th volume with [0,0,0] for non–diffusion–weighted volumes.

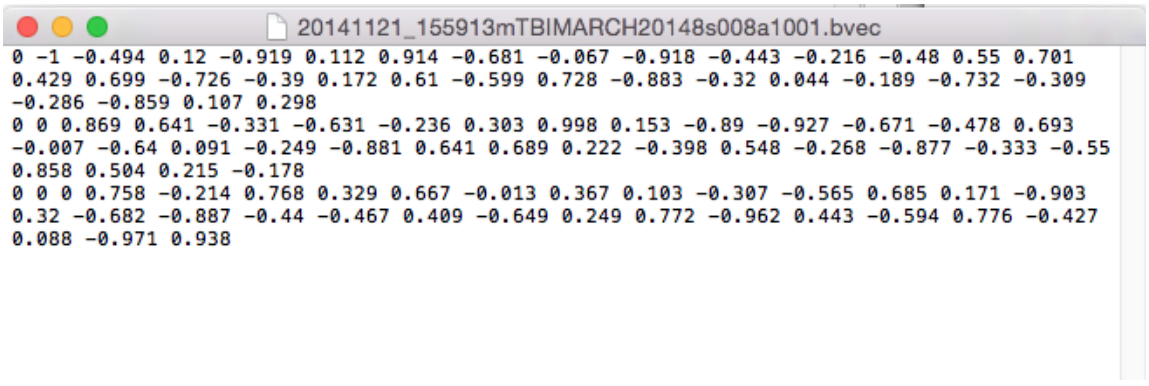

Figure 3.1: bvec

The bval file contains the b–values (in s/mm^2) corresponding to the volumes in

the relevant Nifti file), with 0 designating non–diffusion–weighted volumes, space–delimited.

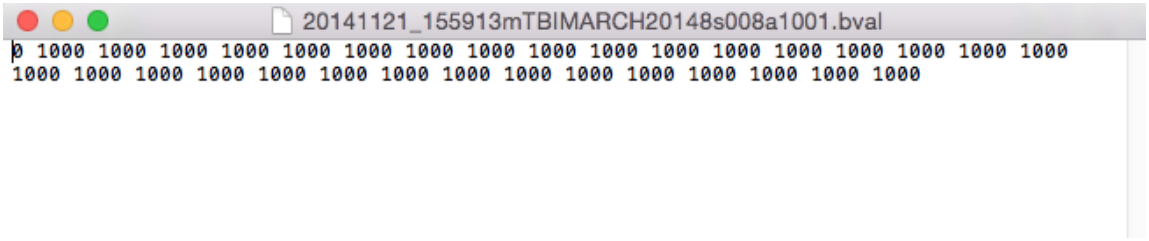

Figure 3.2: bval

So the first step that we did after acquiring the DWI images is called topup[40] using FSL. As of now, top up is still a command line tool and is not yet available through the graphical user interface. Diffusion imaging is typically performed using diffusion weighted spin-echo EPI images. These images will be very sensitive to non-zero off-resonance fields. Such fields will be caused by the susceptibility distribution of the subjects head (known as a susceptibility-induced off-resonance field) and by eddy currents (EC) from the rapid switching of the diffusion weighting gradients (known as an eddy current-induced off-resonance field). In addition to that a diffusion protocol can be quite long, making it almost inevitable that the subject will move.

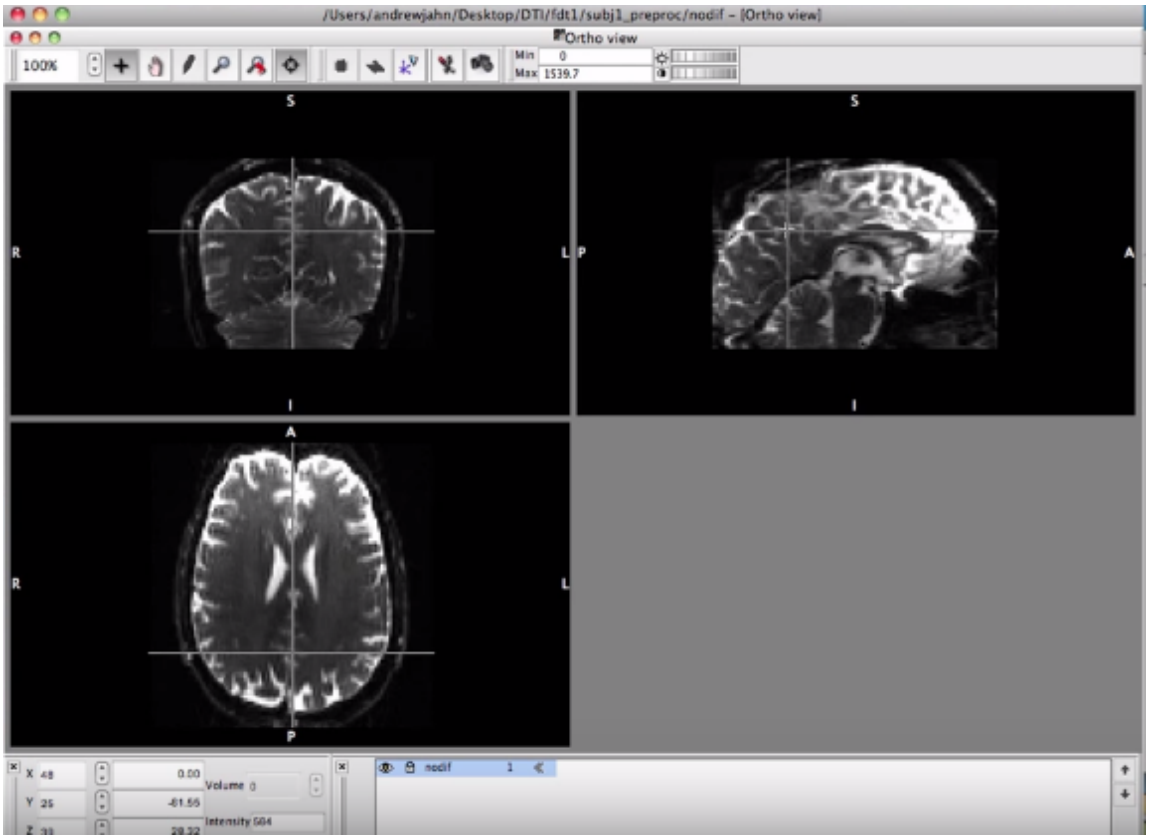

Figure 3.3: NIFTI Image Visualization in FSLview for Subject 007

The susceptibility induced field will be (to a first approximation) constant for all the acquired images, which means that the set of images will be internally consistent. It is a problem mainly because it will cause a geometric mismatch between the structural images (which are typically unaffected by distortions) and the diffusion image. Topup is a tool for estimating the susceptibility induced field. In order to estimate and correct also for EC-induced distortions one will either need to run a tool like e.g. $_{eddy_correct}$ prior to running $_{applytopup}$. Or one can feed the output from $_{topup}$ into the eddy tool.

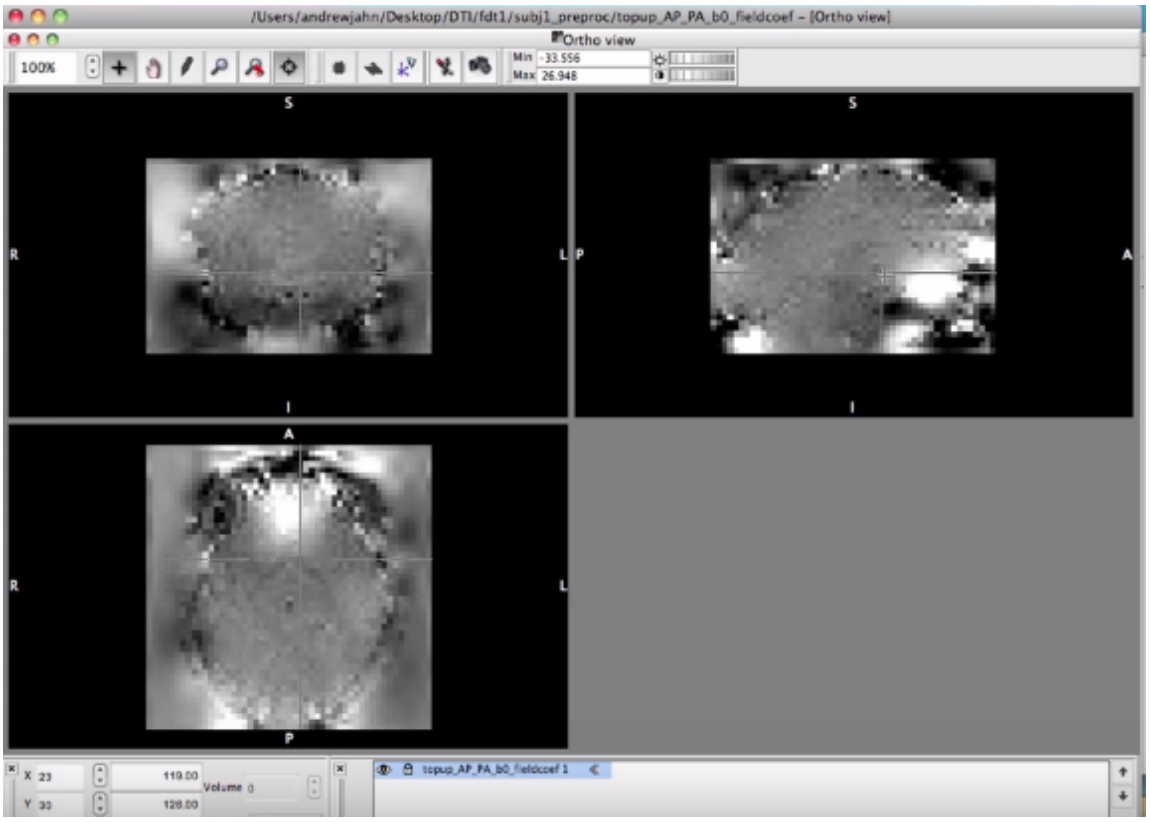

Figure 3.4: Error estimation areas after running the topup command (for subject 007)

The blurry areas in Figure 3.4 indicate places where distortion occurred. After running the *applytopup*, we obtained an almost error-free image. These steps were performed for every individual dataset.

The method that *topup* uses to find the susceptibility off-resonance field is to use two, or more, acquisitions where the acquisition parameters are different so that the mapping field→ distortions are different. A typical example of this is two acquisitions with opposing polarities of the phase-encode blips which means that the same field leads to distortion going in opposing directions in the two acquisitions.

Given the two images and knowledge of the acquisition parameters topup will then attempt to estimate the field by finding the field that when applied to the two volumes will maximise the similarity of the unwrapped volumes. The similarity is gauged by the sum-of-squared differences between the unwrapped images. This measure allows us to use Gauss-Newton for jointly finding the field and any movement that may have occurred between the two acquisitions.

FSL is a comprehensive library of analysis tools for FMRI, MRI and DTI brain imaging data. It runs on Apple and PCs (both Linux, and Windows via a Virtual Machine), and is very easy to install. Most of the tools can be run both from the command line and as GUIs ("point-and-click" graphical user interfaces)[41].

3.3 Processing and Visualization

After correcting our images, we had to visualize and process them. in this step, we used MedInria[42], which is a multi-platform medical image processing and visualization software. The steps taken were as follow:

- Loading the preprocessed image into MedInria

- Estimating the model by choosing the DTI estimation Algorithm, uploading the bvec file as the gradient, then pressing "Estimate Model" in the model estimation toolbox Figure 3.5 will give us a model estimate shown in Figure 3.6.

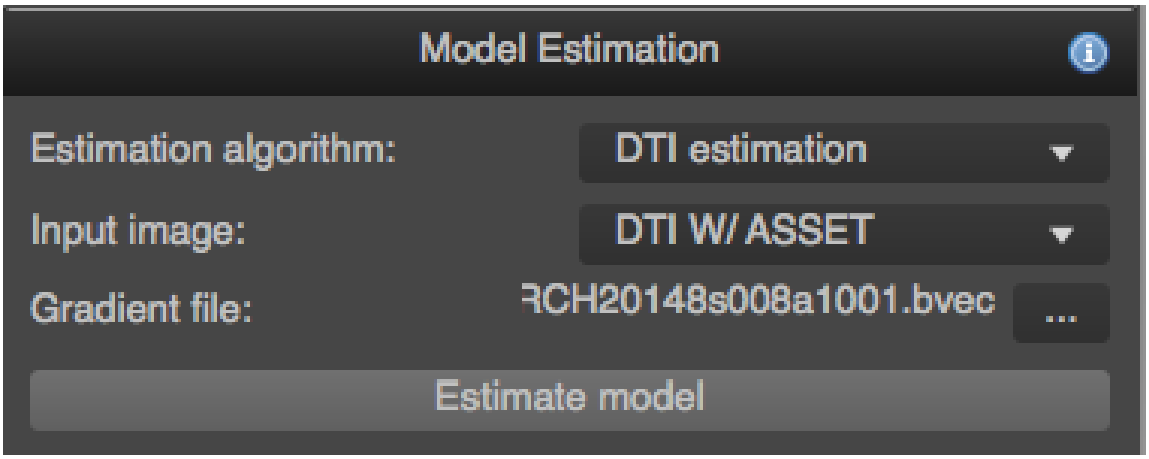

Figure 3.5: Model estimation Toolbox

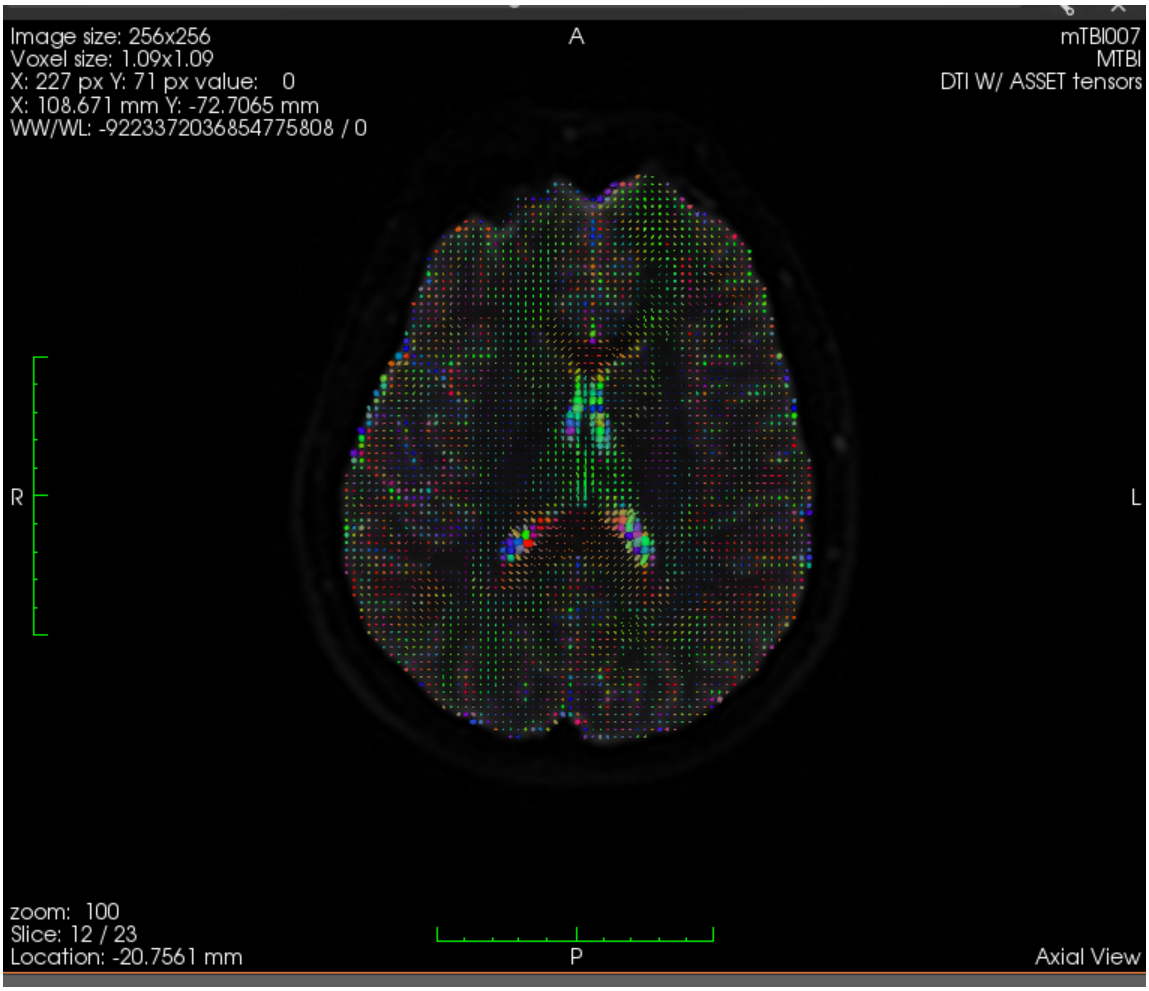

Figure 3.6: Estimated DTI Model in MedInria

- Choosing a DTI scalar map in the diffusion scalar maps toolbox as shown in Figure 3.7. In our case we chose ***FA (with a colored brain behind)*** or **Colored Fractional Anisotropy**.

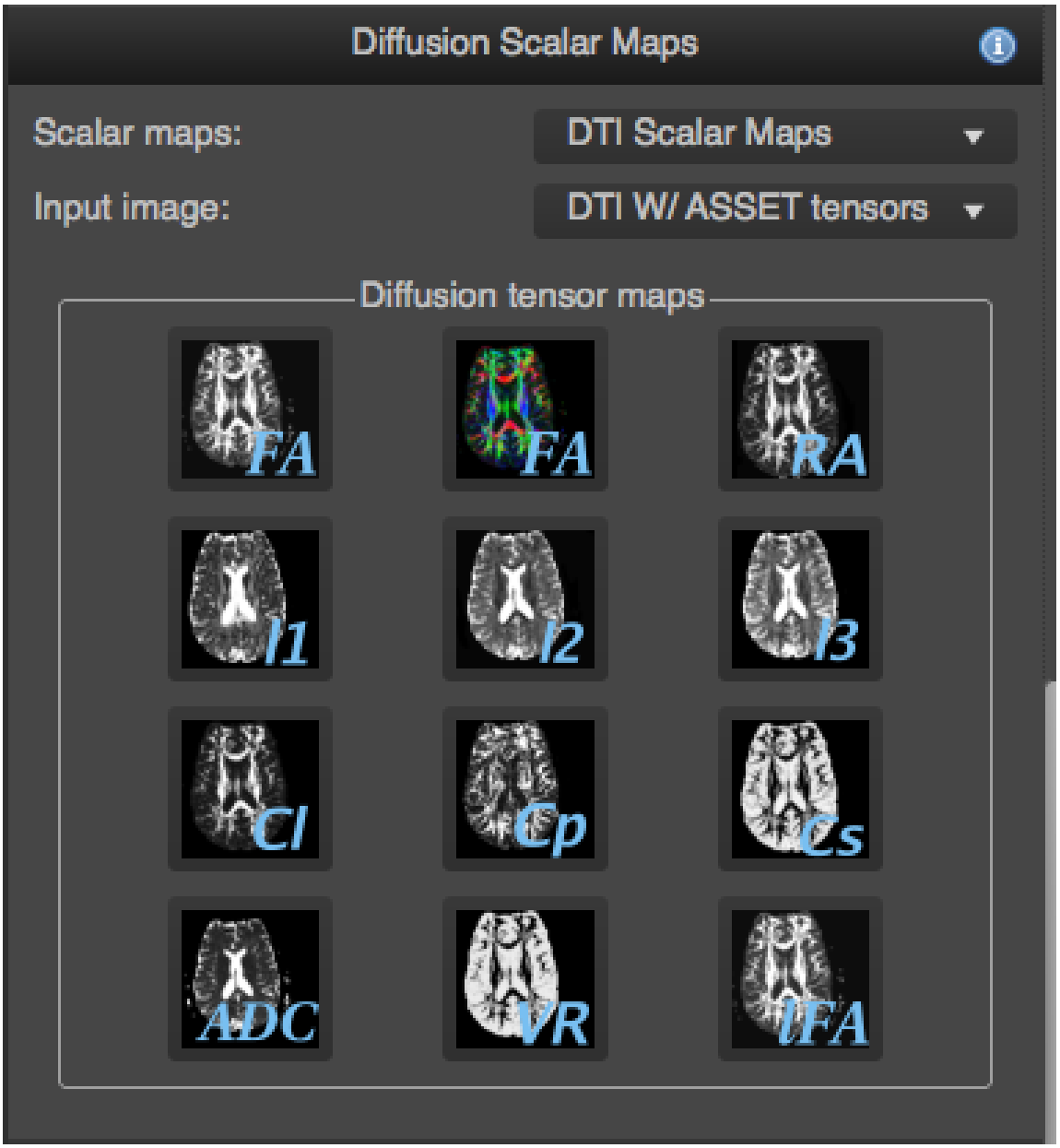

Figure 3.7: Scalar maps toolbox

- Tractography: We ran the tractography algorithm in the tractography toolbox shown in Figure 3.8.After a few seconds, we obtain white-matter tracts in form of fiber bundles shown in Figure 3.9. These tracts use the RGB color coding in

which red represents fibres crossing from left to right, green represents fibers traversing in anterior-posterior direction, and blue represents fibers going from superior to inferior.

Several parameters can be tweaked before running the algorithm:

- Starting FA threshold and Stopping FA threshold: In order to build the fibers, the algorithm starts by seeding one in every voxel whose FA value is higher than "Starting FA threshold" and stops its construction when it reaches a voxel with FA value lower than "Stopping FA threshold".

- Smoothness: The smoothness value indicates how "strictly" the fiber follows the tensors. The higher the value, the less the fiber gets deviated by the tensors. A value of 0 indicates that the fiber strictly follows the tensors.

- Minimum length:At the final stage of the algorithm, fibers whose length is below the chosen amount (in millimetres) are deleted.

- Sampling:If seeding a fiber in every voxel allowed by the FA threshold is not desired, the sampling feature will force the algorithm to only seed one fiber in every X voxels, being X the selected sampling value.

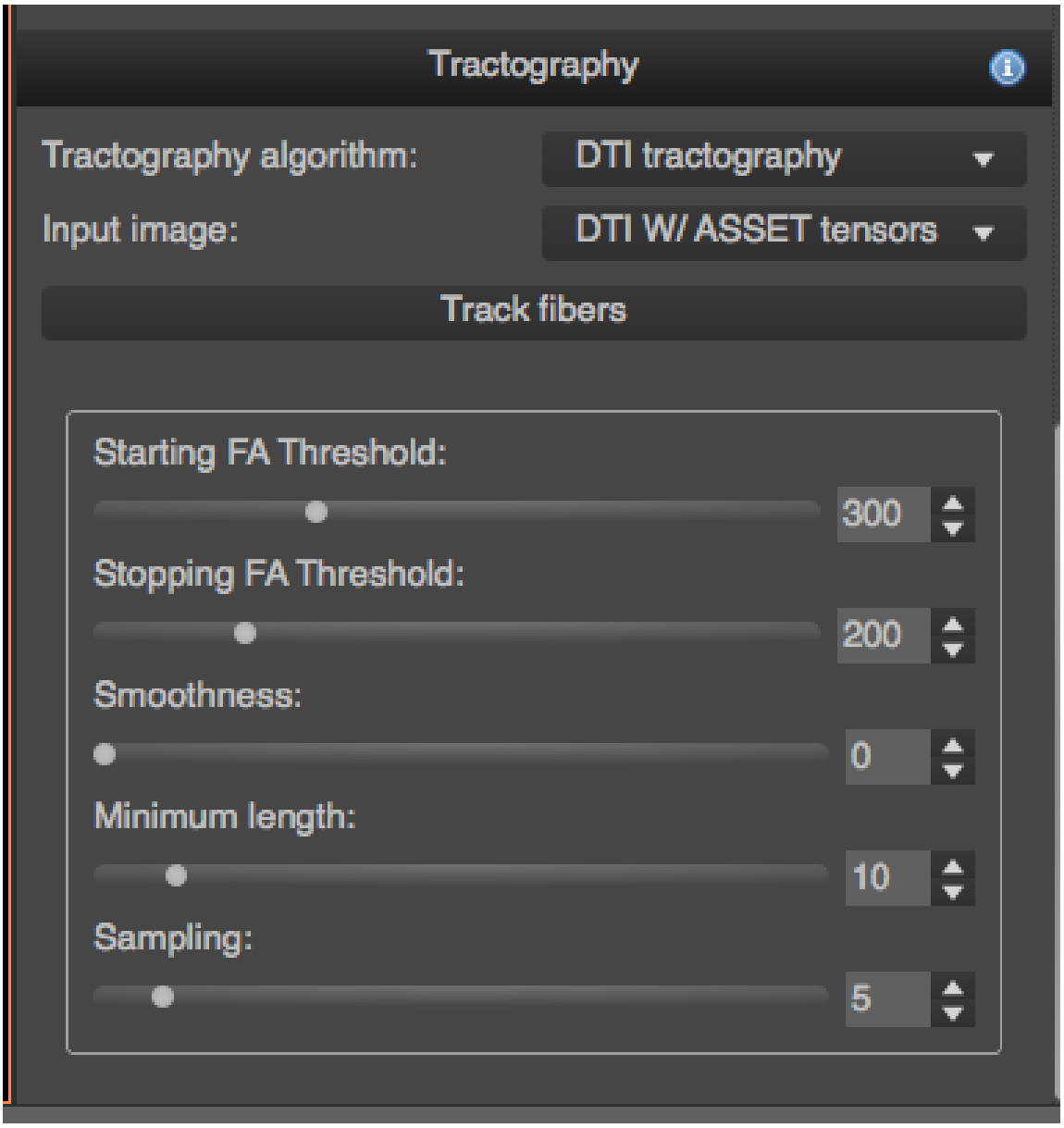

Figure 3.8: Tractography Toolbox

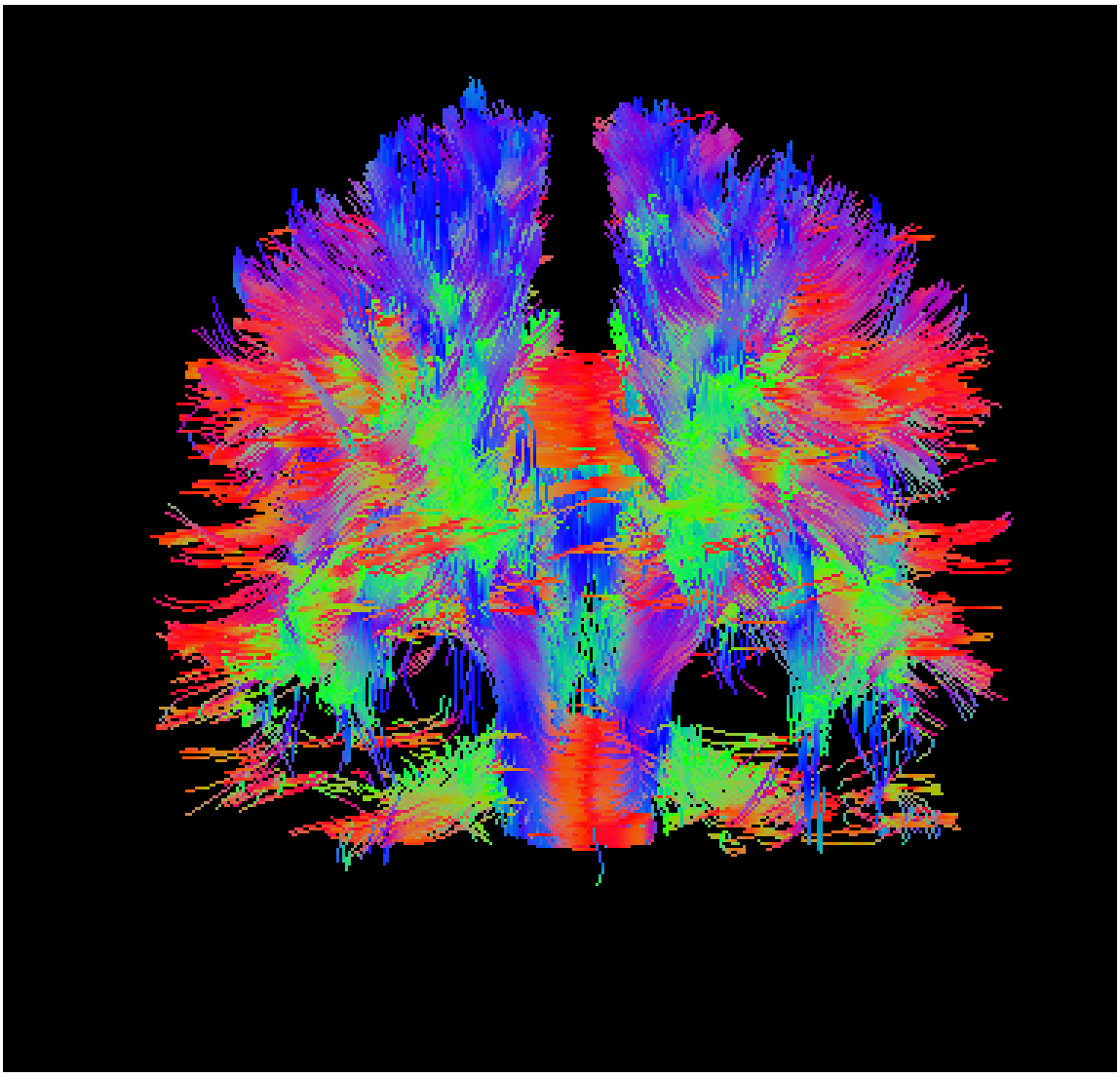

Figure 3.9: White-matter fiber Bundles in RGB format

3.4 Quantitative Analysis: Region of Interest (ROI) Analysis

After obtaining the fiber tracts, we had to do a quantitative analysis, and for this, we chose to perform a Region of Interest(ROI) analysis. We divided the analysis in

two parts:

- We created binary masks using FSL.
- We used those masks to create regions of interest
- We measured FA and ADC for all 20 regions of all the datasets individually
- We separated the control subjects from the patients and performed a group analysis using SAS.
- We performed a simple Z score test in MATLAB to compare each subject to the average, and where there is a significant difference in FA and ADC individually.

3.4.1 Binary Masks Creation

To create binary masks, we used the JHU white-matter tractography atlas [7]. This atlas has 20 structures that were identified probabilistically by averaging the results of running deterministic tractography on 28 normal subjects (mean age 29, M:17, F:11).

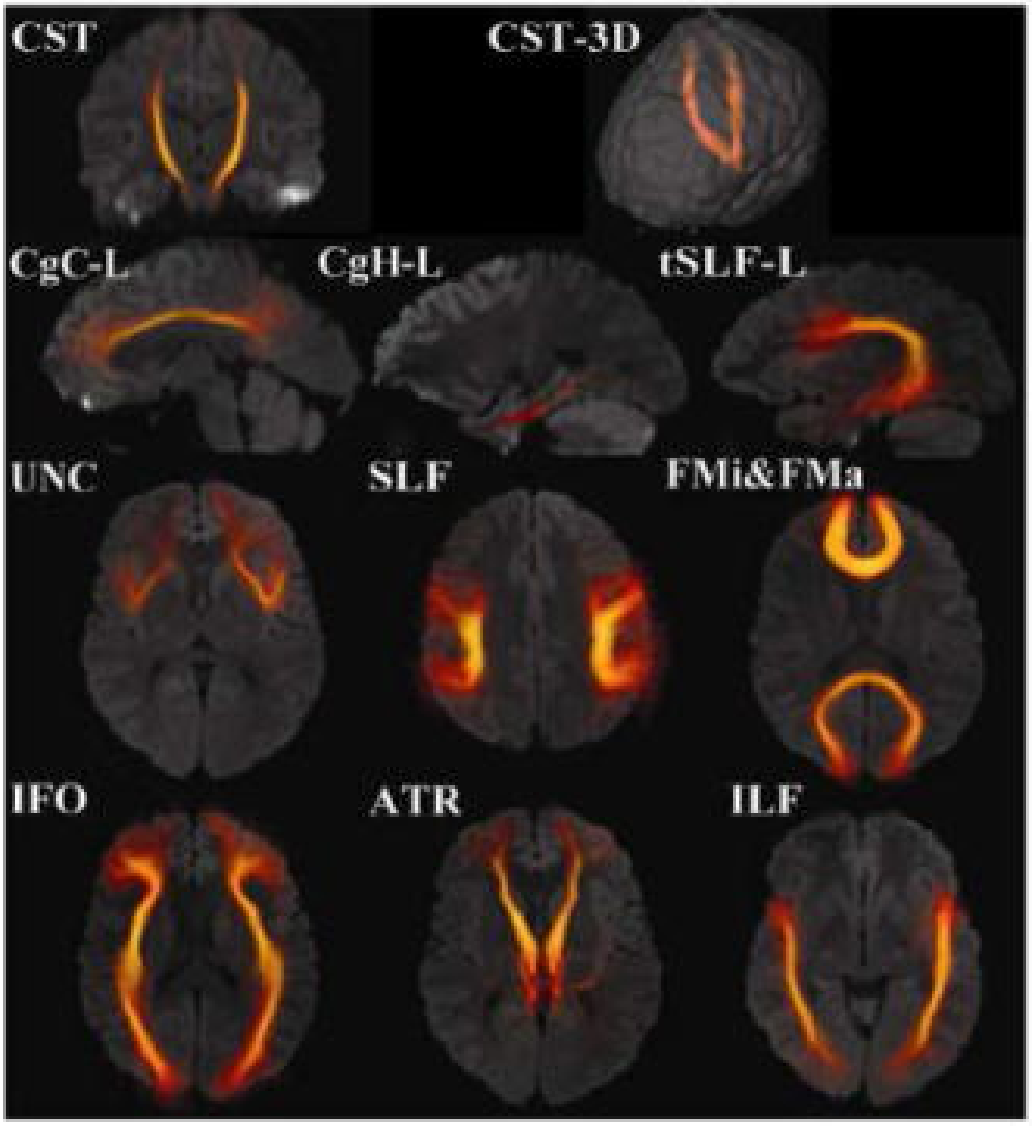

Figure 3.10: JHU White-matter Tractograhy Atlas. Abbreviations are: ATR: anterior thalamic radiation; CgC: cingulum in the cingulated cortex area; Cgh: cingulum in the hippocampal area; CST: cortitospinal tract; FMa: forceps major; FMi: forceps minor; IFO: inferior fronto-occipital fasciculus; SLF: superior longitudinal fasciculus; tSLF: the temporal projection of the SLF; UNC: uncinate fasciculus [7].

FSL was used to create 20 regions of interests based on this atlas.

3.4.2 ROI quantitative Analysis

After the tractography, each ROI was imported into MedInria for a quantitative analysis. Each ROI was validated respectively and we got FA, ADC, and the Lengths of fibers.

3.4.3 Group Analysis

The group analysis was performed using the Statistical Analysis Software (SAS)[43]. We used **proc glm** to run the one-way MANOVA with p value set at 0.05, corrected for multiple comparisons, considering group and visit as the independent variables and individual regions as dependant variable. The one-way MANOVA was performed for the two DTI measures, namely FA and ADC.

The SAS System

The GLM Procedure

Class Level Information		
Class	Levels	Values
Visit_ID	3	1 2 3
Group_ID	2	1 2

Number of Observations Read	40
Number of Observations Used	40

Figure 3.11: The GLM Procedure on SAS system

The output above indicates that there are three variable listed on the class statement, group, Visit_ID (3 levels of value 1,2,3), and Group_ID (2 levels of value 1(for patients) and 2 (for control subjects)) has three levels. We also see that 40 observations in the dataset were used in the analysis.

3.4.4 Z-score tests

Finally, a simple standard Z-Score was performed in MATLAB to see where the major differences in FA and ADC were for each patient, compared to the group of

control subjects. The z score formula used and the threshold is

$$z = \frac{X - \mu}{\sigma} \tag{3.1}$$

where X is our current FA or ADC measured, μ is the mean FA or ADC for the control subjects, and σ is the standard deviation of FA or ADC.

Chapter 4

Results

In this chapter the results of the data analysis are presented. The data were collected and then processed in response to the problems posed in chapter 1 of this thesis. Two fundamental goals drove the collection of the data and the subsequent data analysis. The first goal was to see see if we could detect areas of injury, and the second was if we could see an improvement on the subsequent visits.These objectives were accomplished. The findings presented in this chapter demonstrate the potential for merging theory and practice.

4.1 Group Analysis

This analysis was performed to see whether there was a significant difference in FA and ADC between the group of patients, group 1, and the group of control subjects, group 2. The analysis was performed per region of interest, hence we had 20 results for each.The table of legend of the regions of interests is given in table 4.1.

Table 4.1: Legend of regions of interest numbers and their names

Region	Name
1	Left Anterior Thalamic Radiation (ATR-L)
2	Right Anterior Thalamic Radiation (ATR-R)
3	Left Corticospinal Tract (CST-L)
4	Right Corticospinal Tract (CST-R)
5	Left cingulum in the cingulated cortex area (CgC-L)
6	Right cingulum in the cingulated cortex area (CgC-R)
7	Left cingulum in the hippocampal area (CgH-L)
8	Right cingulum in the hippocampal area(CgH-R)
9	forceps major (FMa)
10	forceps minor (FMi)
11	Left inferior fronto-occipital fasciculus (IFO-L)
12	Right inferior fronto-occipital fasciculus (IFO-R)
13	Left Inferior Longitudinal Fasciculus (ILF-L)
14	Right Inferior Longitudinal Fasciculus (ILF-R)
15	Left Superior Longitudinal Fasciculus (SLF-L)
16	Right Superior Longitudinal Fasciculus (SLF-R)
17	Left Uncicate Fasciculus (UNC-L)
18	Right Uncicate Fasciculus (UNC-R)
19	Left temporal projection of the SLF(tSLF-L)
20	Right temporal projection of the SLF (tSLF-R)

The regions above look like figure 4.1

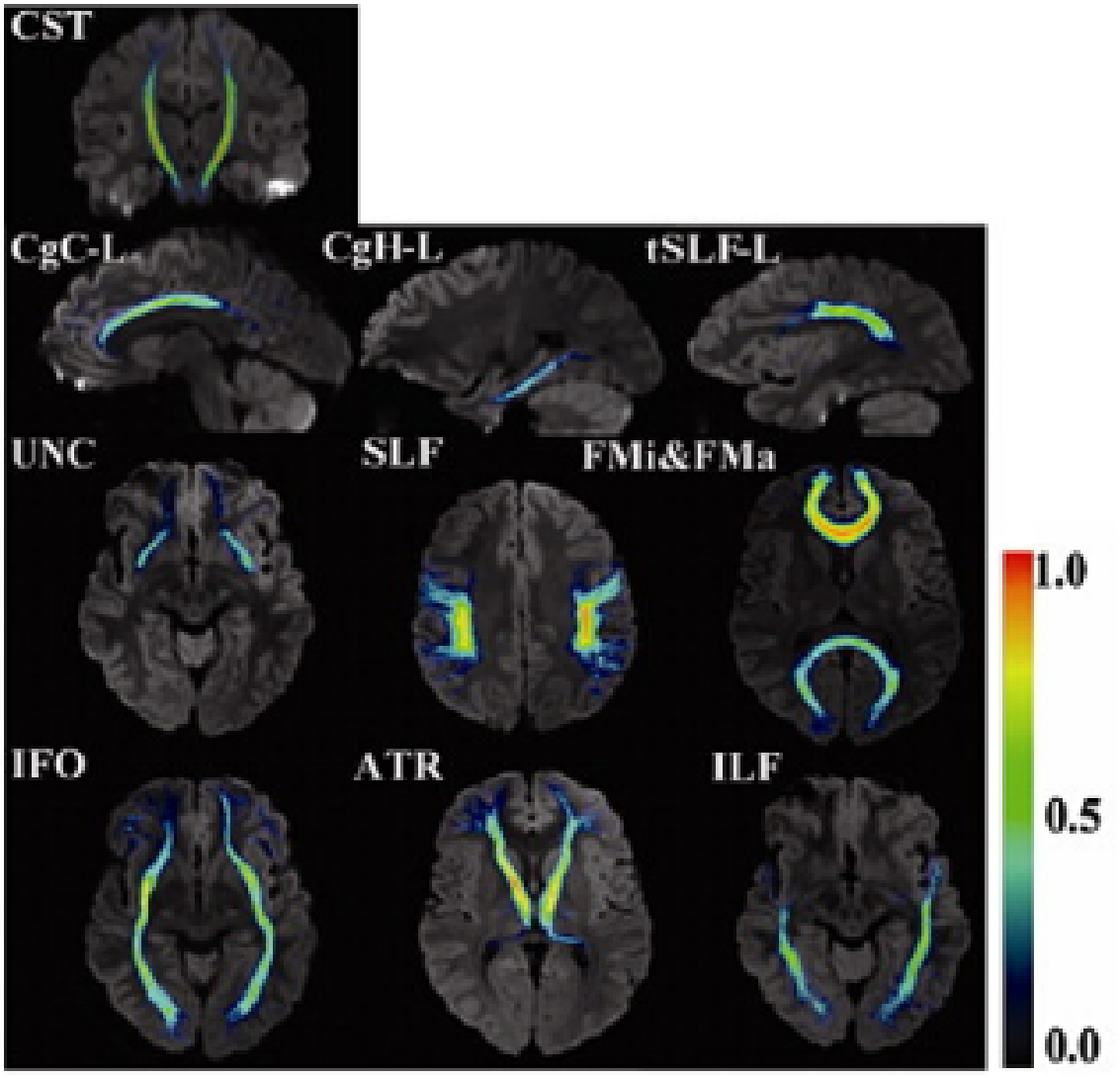

Figure 4.1: JHU White-Matter Tractography Atlas where color-scaled probabilistic maps are superimposed on 2D slices.The color represents probability, as shown in the color bar [7].

4.1.1 Fractional Anisotropy

The outputs of our **proc glm** show that region 15 was statistically different FA, while others were not.

Source	DF	Type I SS	Mean Square	F Value	Pr > F
Visit_ID	2	0.00095428	0.00047714	1.96	0.1558
Group_ID	1	0.00148508	0.00148508	6.11	0.0186
Visit_ID*Group_ID	2	0.00082336	0.00041168	1.70	0.1987

Source	DF	Type III SS	Mean Square	F Value	Pr > F
Visit_ID	2	0.00061761	0.00030880	1.27	0.2934
Group_ID	1	0.00151021	0.00151021	6.22	0.0177
Visit_ID*Group_ID	2	0.00082336	0.00041168	1.70	0.1987

Figure 4.2: SS1 and SS3 output of SAS showing F<P_r(0.05) for the Group_ID for region 15

.

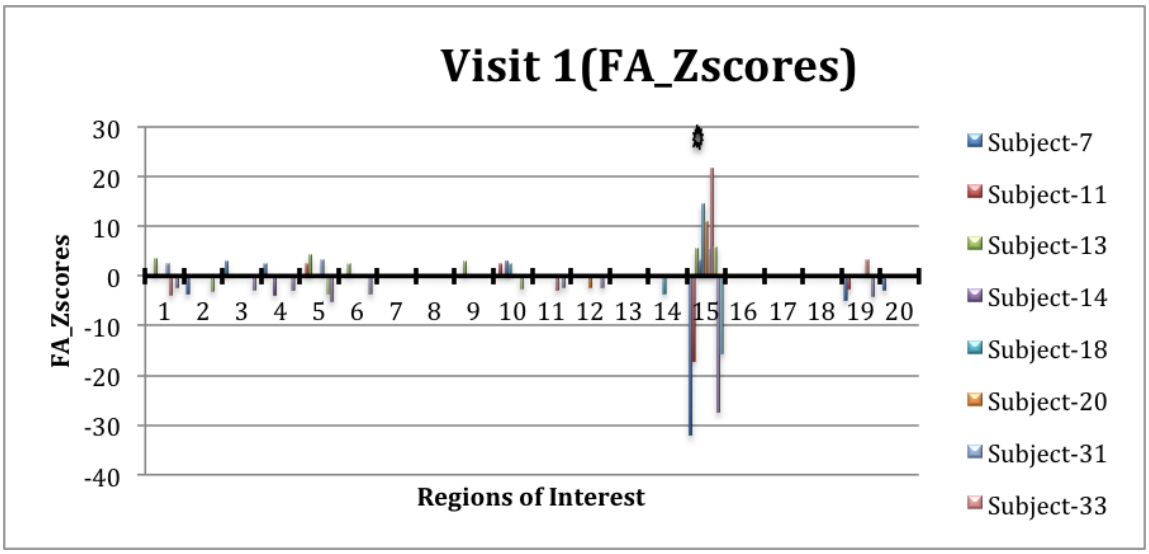

Figure 4.3: FA Z–Scores VS Regions of interest for all Subjects; Visit 1.

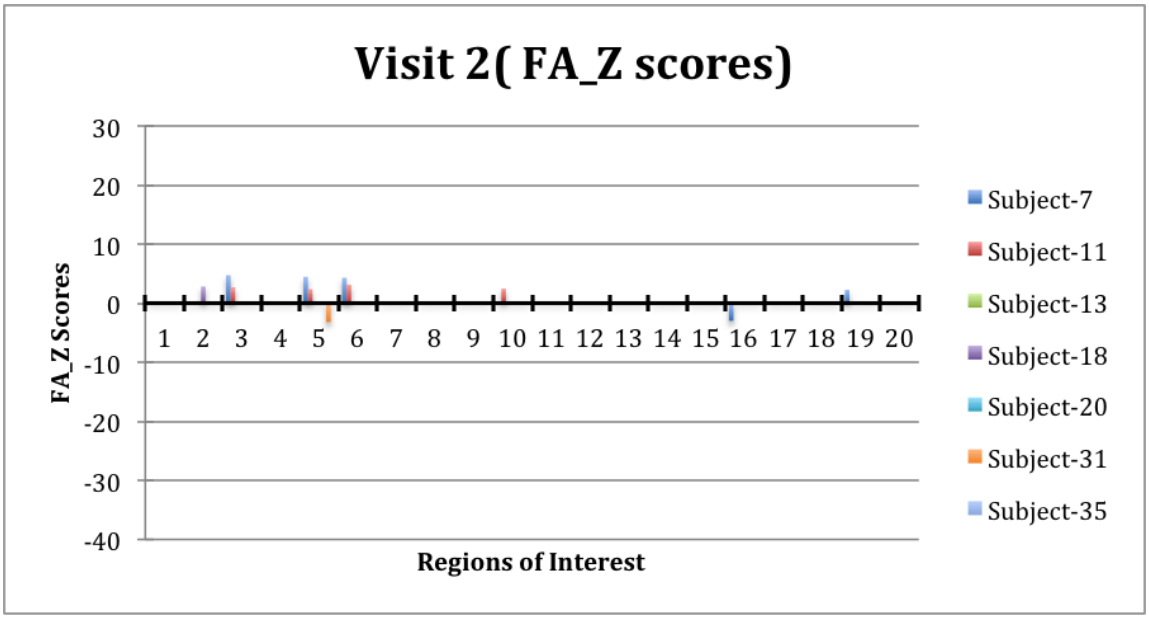

Figure 4.4: FA Z–Scores VS Regions of interest for all Subjects; Visit 2

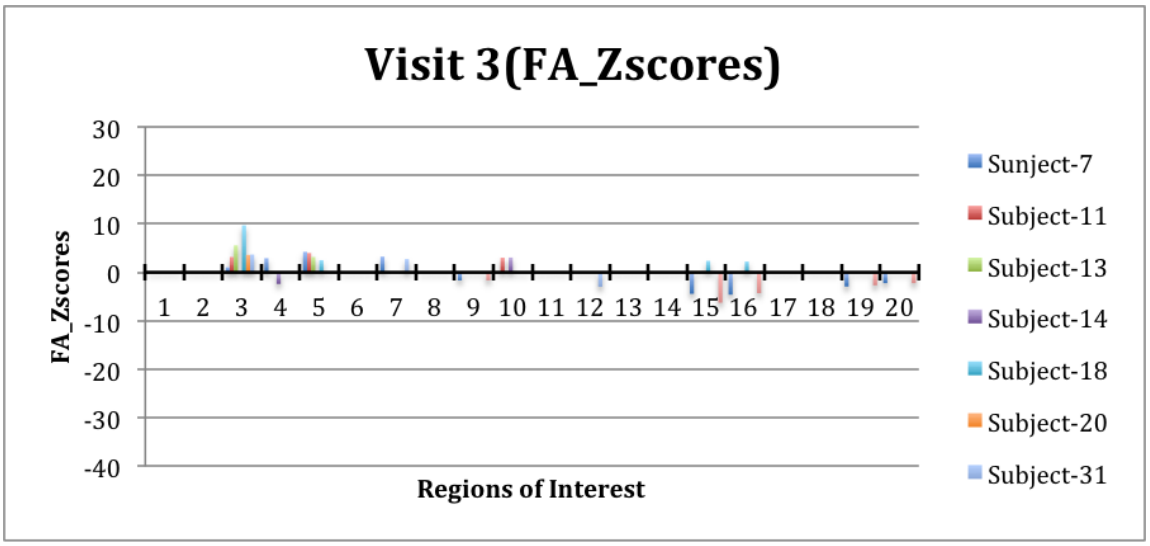

Figure 4.5: FA Z–Scores VS Regions of interest for all Subjects; Visit 3

From the graphs above, we see that there was a significant difference in FA in region 15 (Left Superior Longitudinal Fasciculus (SLF-L)) for all subjects on their first visit following the injury. We also see minor differences in other regions as well. We observe that during the subsequent visits, there was an improvement in FA for most patients. The detailed results per patient will be given in the sections below.

4.1.2 Apparent Diffusion Coefficient

The outputs of our **proc glm** show that there was no statistical difference in ADC between the two groups for all 20 regions.

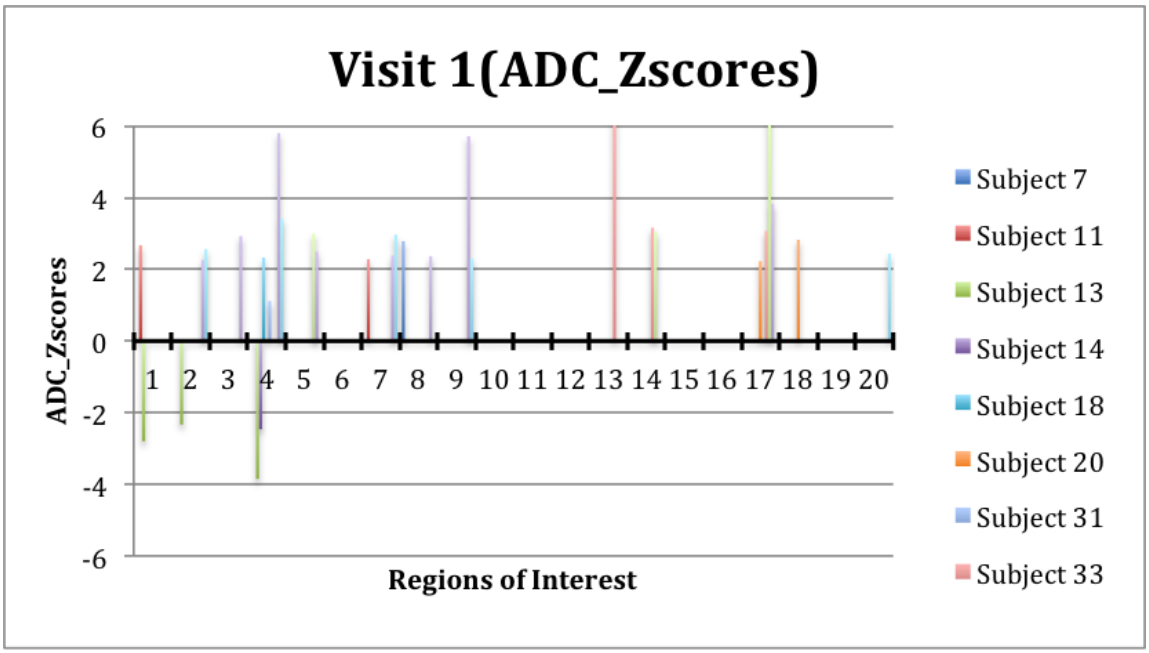

Figure 4.6: ADC Z–Scores VS Regions of interest for all Subjects; Visit 1

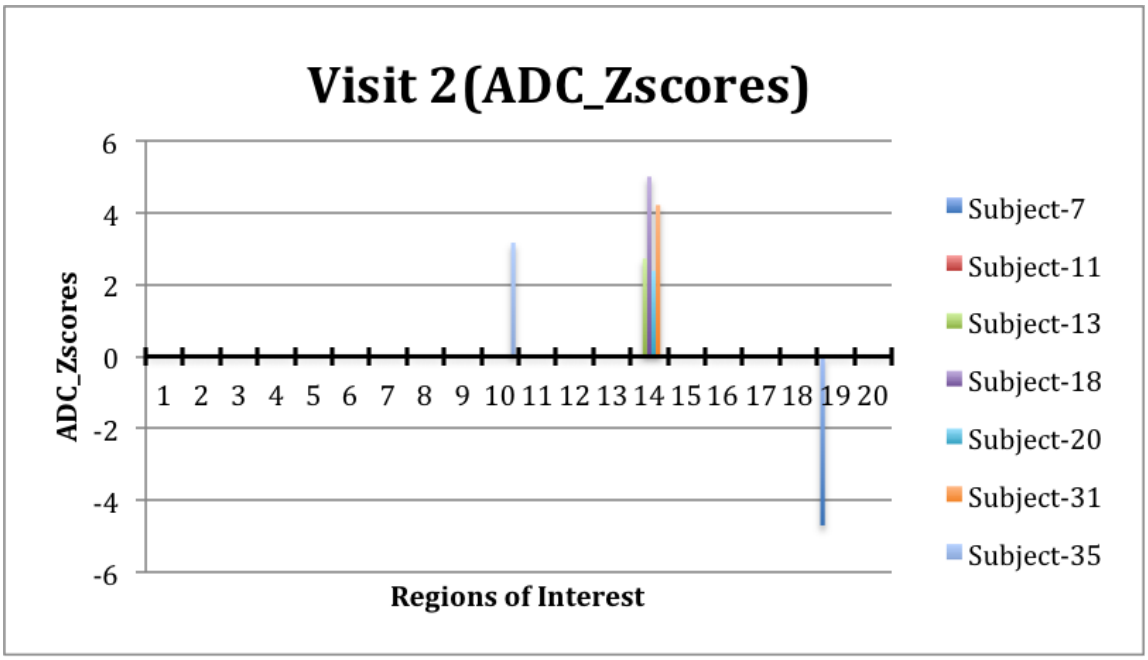

Figure 4.7: ADC Z–Scores VS Regions of interest for all Subjects; Visit 2

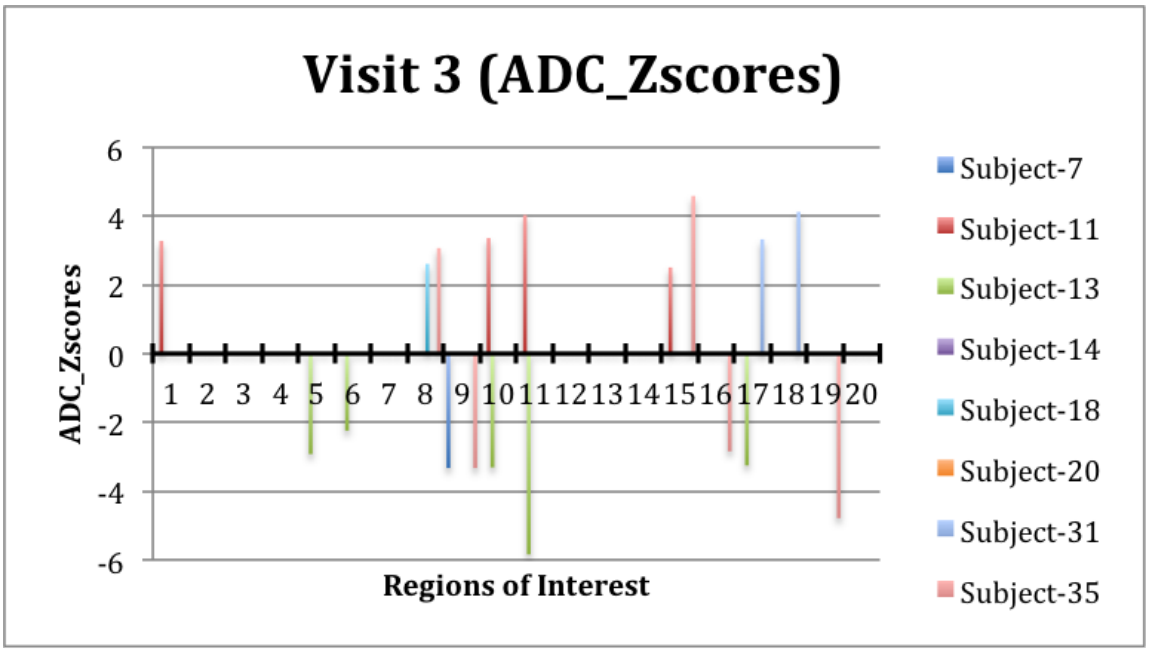

Figure 4.8: ADC Z–Scores VS Regions of interest for all Subjects; Visit 3

As the group analysis performed in SAS showed, there wasn't any significant difference in ADC between the Control subjects and the patients. The bars showing in the previous graphs only show a minor difference in ADC for all subjects. Again, detailed results will be given in the following sections.

4.2 Individual Analysis using Z-scores

After performing a group analysis, we wanted to show how each subject's injury looked like on his/her first visit, and if they recovered in the following visits. We proceeded by first giving the medical diagnosis,then we showed the graphs of their FA and ADC for all their visits, and lastly we visualized those abnormalities on the brain using the JHU White-matter tractography Atlas in FSL.

4.2.1 Subject 007 (mTBI patient)

- Medical Diagnosis: the patient had a motorcycle accident and the injury location is on the head, left front.

- Graphs:

  – Fractional Anisotropy: the graph shows that on the first visit, there was a very significant difference in FA in region 15 (Left Superior longitudinal Fasciculus). We can observe improvement in FA in the subsequent visits.

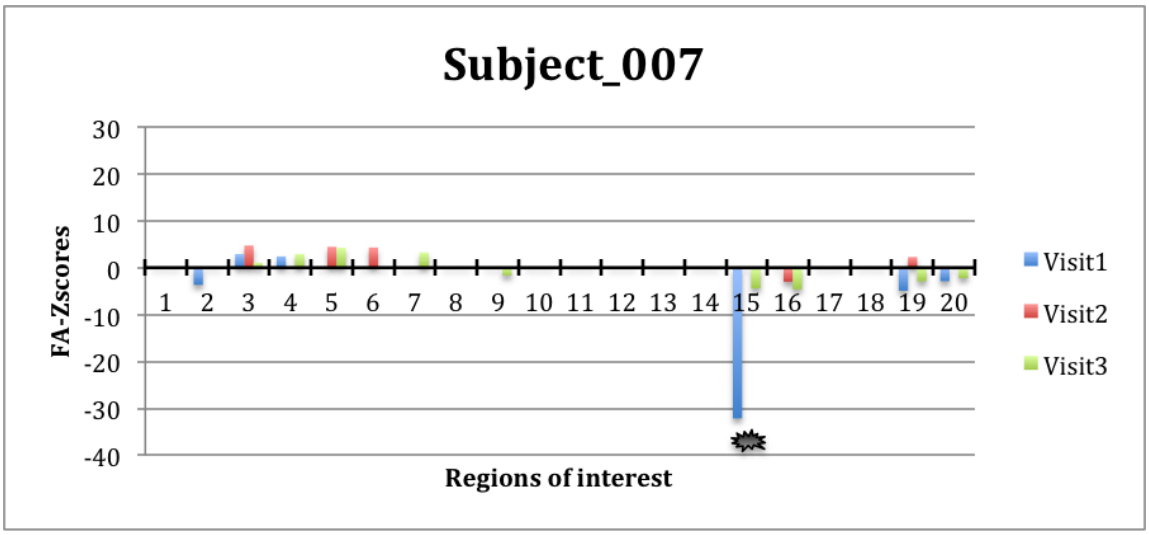

Figure 4.9: FA Z–Scores VS Regions of interest for Subject 007.

  – Apparent Diffusion Coefficient There wasnt any significant difference in ADC but we cannot neglect the fact that there are some differences in some regions.

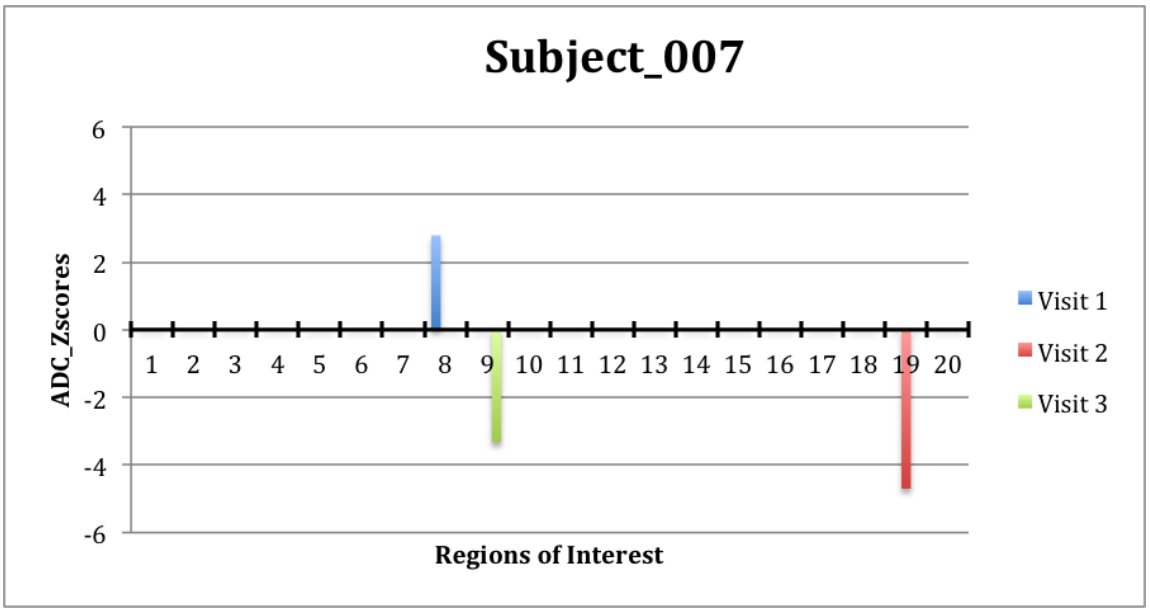

Figure 4.10: ADC Z–Scores VS Regions of interest for Subject 007.

- Visualization: The highlighted parts of the brain show the tracts where the FA of the patient differs from the control subject. We can see an improvement in the following visits.

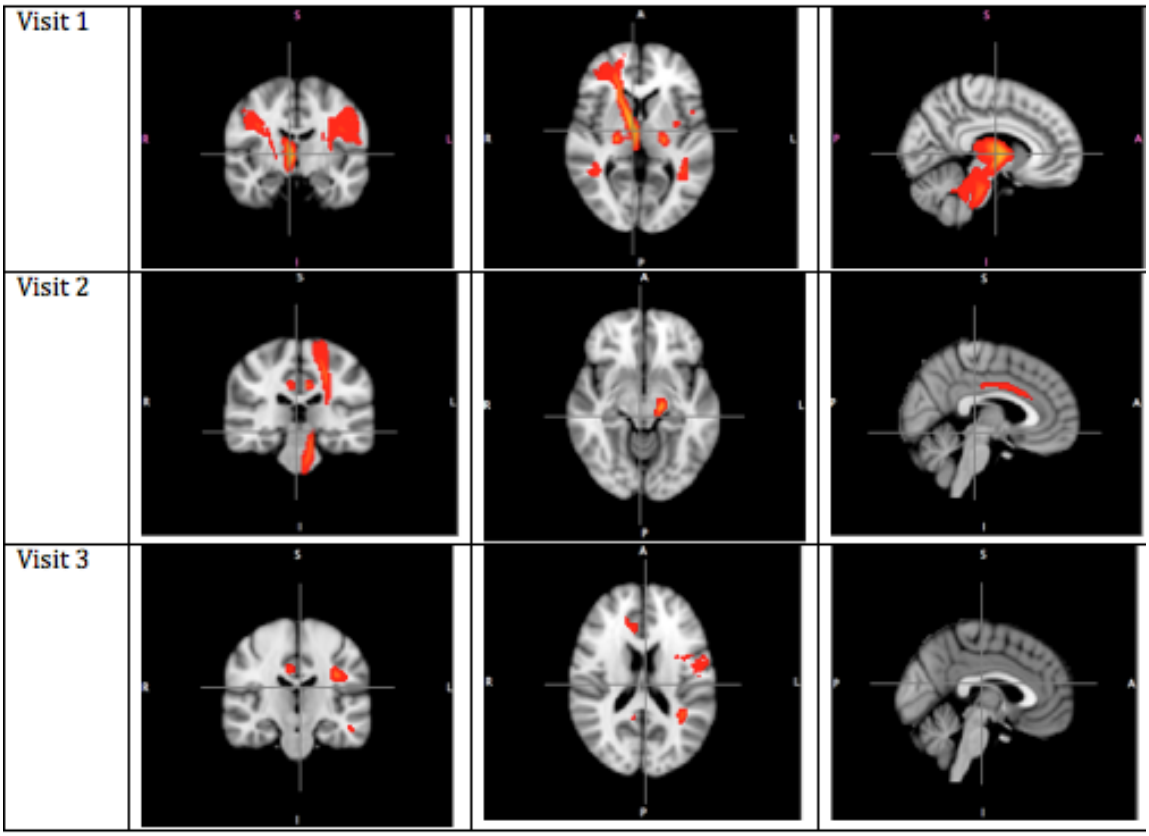

Figure 4.11: FA abnormalities visualizations for all 3 visits

4.2.2 Subject 011 (mTBI patient)

- Medical Diagnosis: the patient fell off the stairs and hit his head and whole right side on concrete.

- Graphs:

  – Fractional Anisotropy: the graph shows that on the first visit, there was a very significant difference in FA in region 15 (Left Superior longitudinal Fasciculus). We can observe improvement in FA in the subsequent visits.

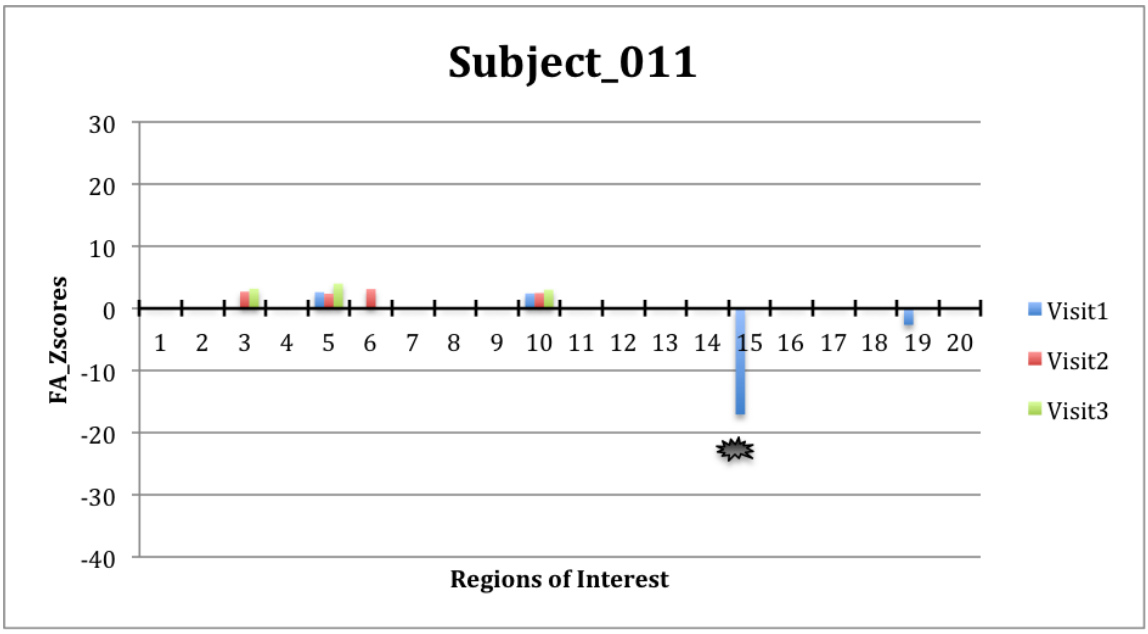

Figure 4.12: FA Z–Scores VS Regions of interest for Subject 011.

– Apparent Diffusion Coefficient There wasnt any significant difference in ADC but we cannot neglect the fact that there are some differences in some regions.

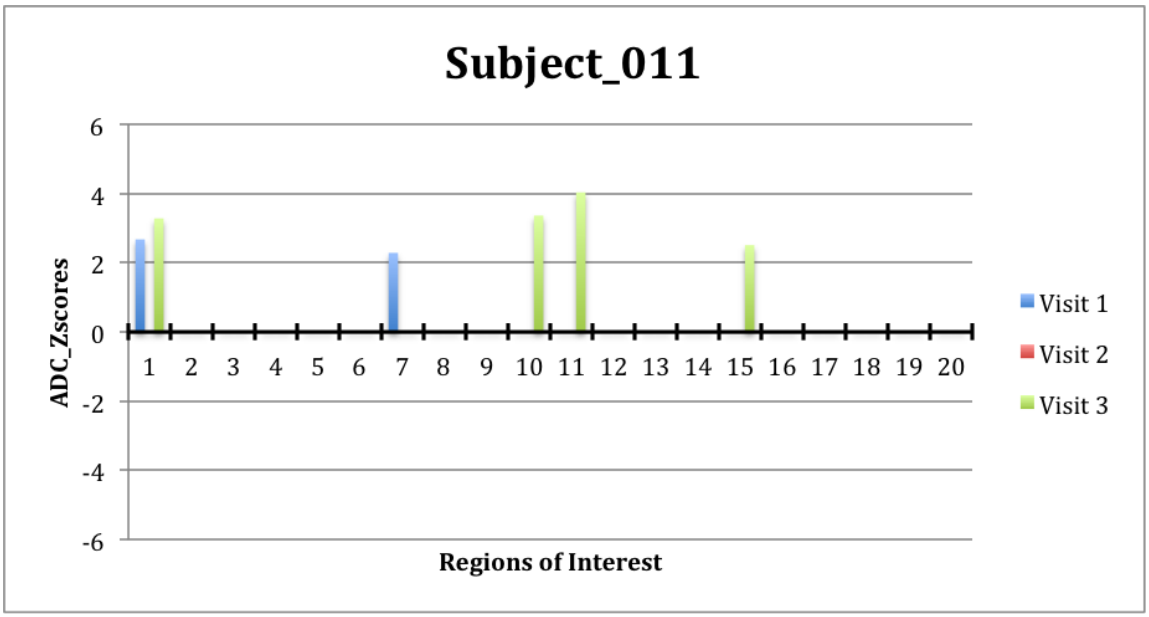

Figure 4.13: ADC Z–Scores VS Regions of interest for Subject 011.

- Visualization: The highlighted parts of the brain show the tracts where the FA of the patient differs from the control subject. We can see an improvement in the following visits.

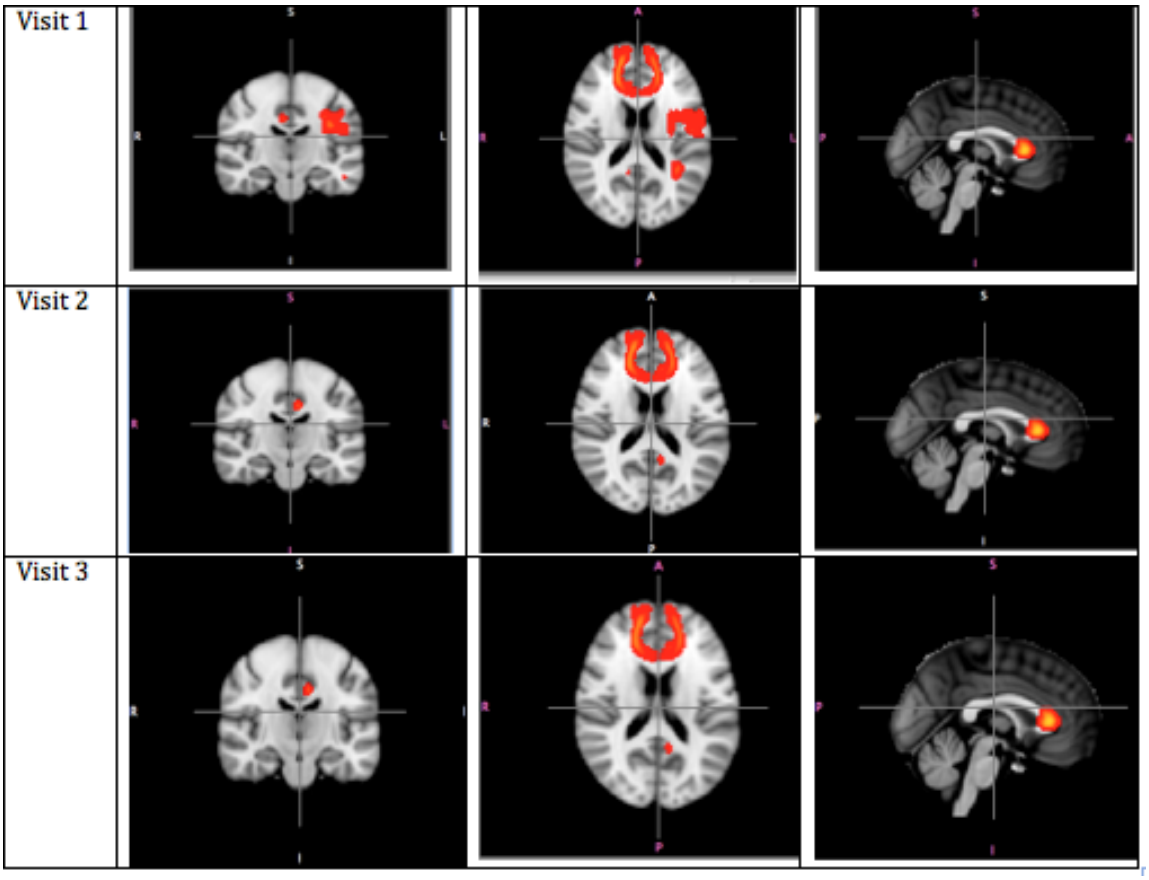

Figure 4.14: FA abnormalities visualizations for all 3 visits

4.2.3 Subject 013 (mTBI patient)

- Medical Diagnosis: the patient fell off the stairs and injured her right leg and her head.
- Graphs:
  - Fractional Anisotropy: From the graph, we can see that there wasnt any significant difference in FA between the patient and the control subject even though there were some minor differences shown.

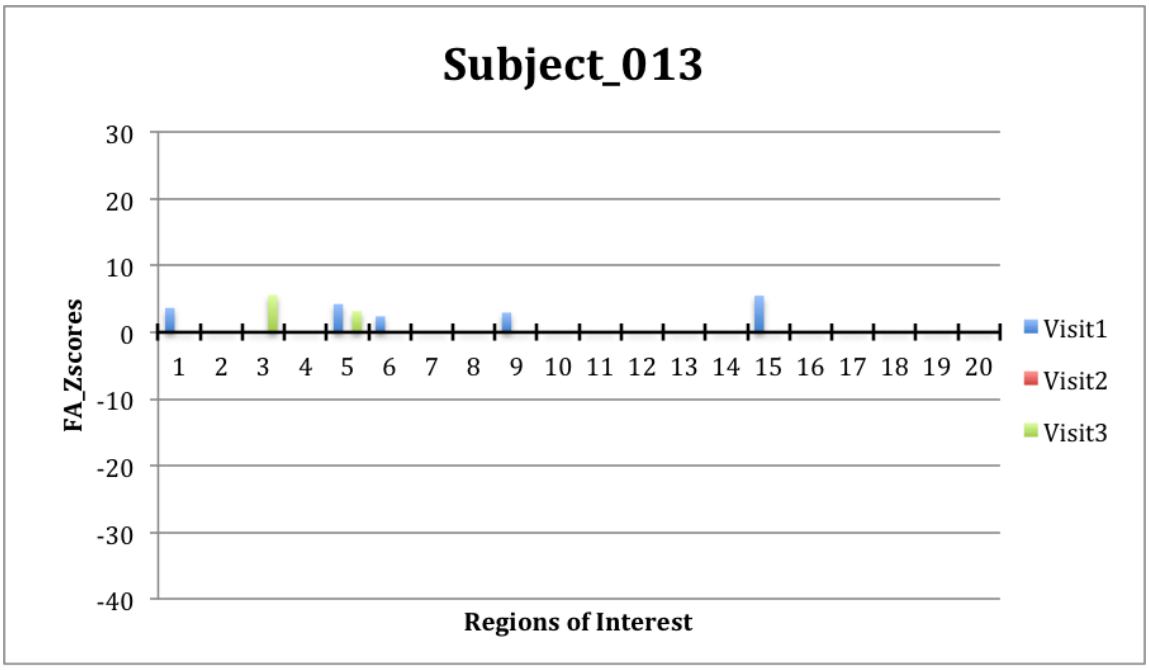

Figure 4.15: FA Z–Scores VS Regions of interest for Subject 013.

– Apparent Diffusion Coefficient: The ADC doesnt show any major statistical difference between the control and the patient. However, the differences here are not negligible.

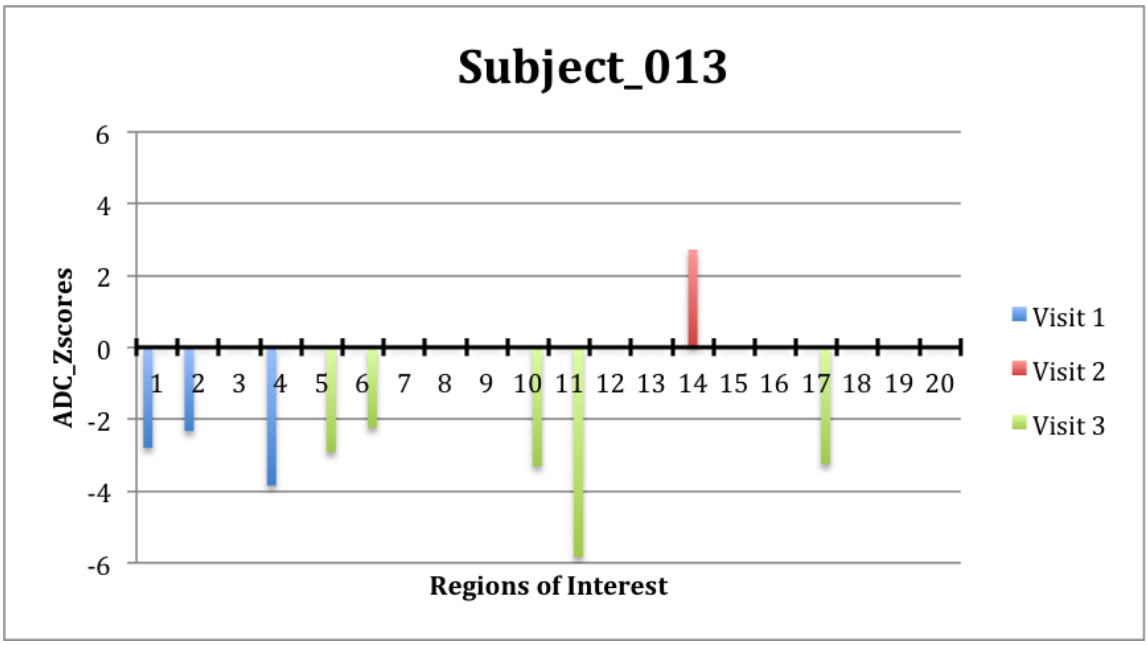

Figure 4.16: ADC Z–Scores VS Regions of interest for Subject 013.

- Visualization: The highlighted parts of the brain show the tracts where the FA of the patient differs from the control subject. We can see an improvement in the following visits.

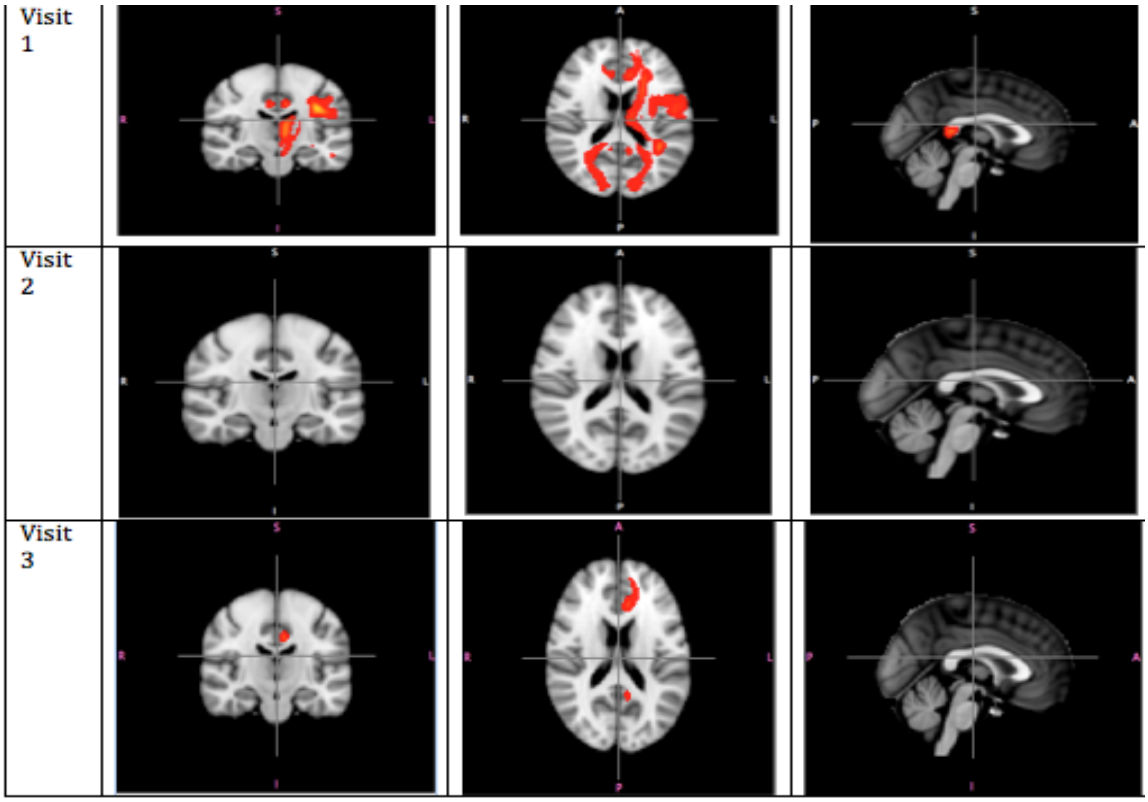

Figure 4.17: FA abnormalities visualizations for all 3 visits

4.2.4 Subject014 (mTBI patient)

- Medical Diagnosis: the patient had an accident and hurt the right front side of his head.

- Graphs:

  – Fractional Anisotropy: From the graph, we can see that there wasnt any significant difference in FA between the patient and the control subject even though there were some minor differences shown.

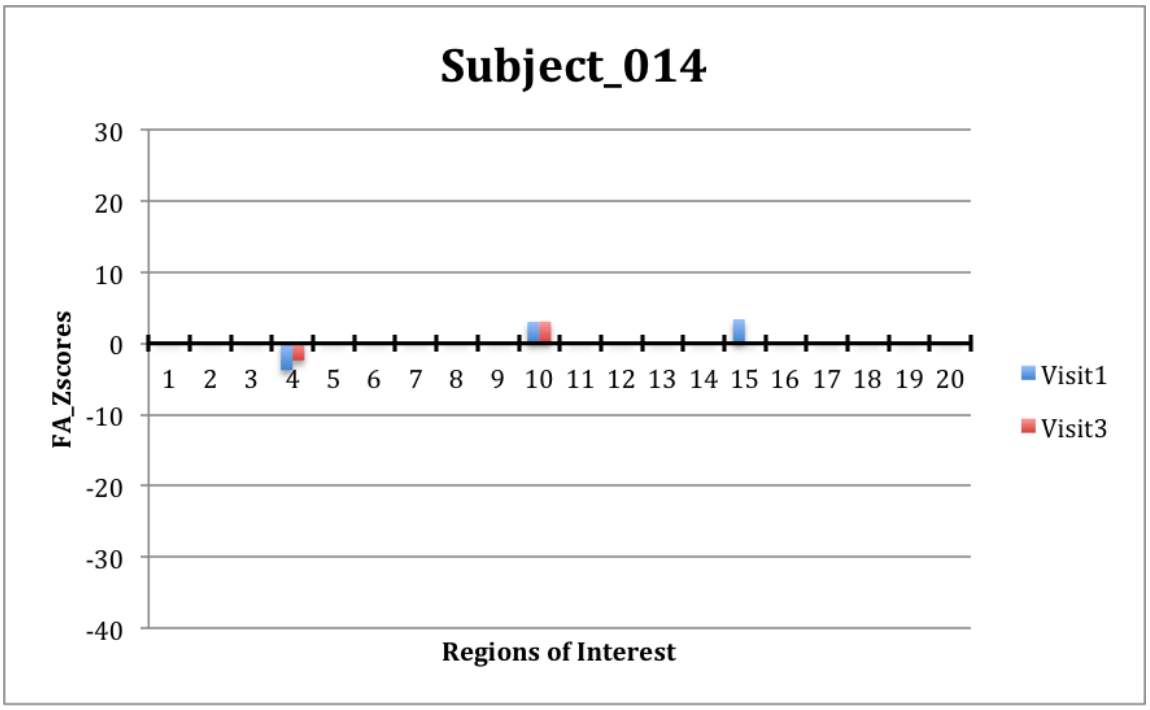

Figure 4.18: FA Z–Scores VS Regions of interest for Subject 014.

– Apparent Diffusion Coefficient: The ADC doesnt show any major statistical difference between the control and the patient. However, the differences here are not negligible.

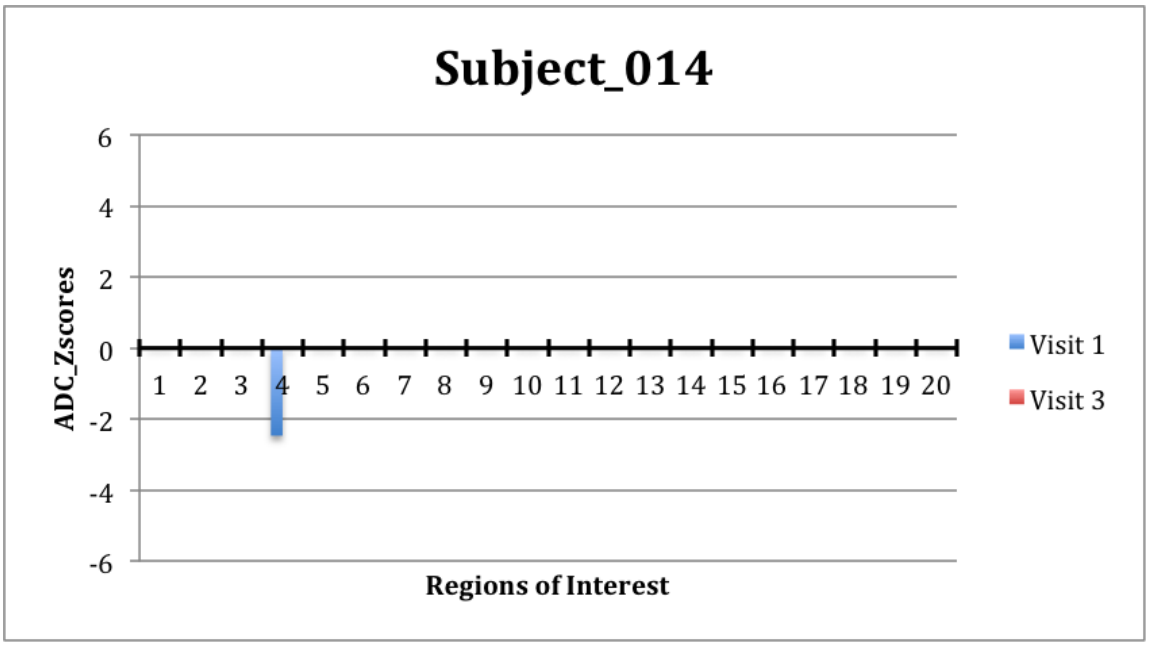

Figure 4.19: ADC Z–Scores VS Regions of interest for Subject 014.

- Visualization: The images below show that the patient was affected on many parts of the brain and it improved on the third visit. This patient did not show up for the second visit.

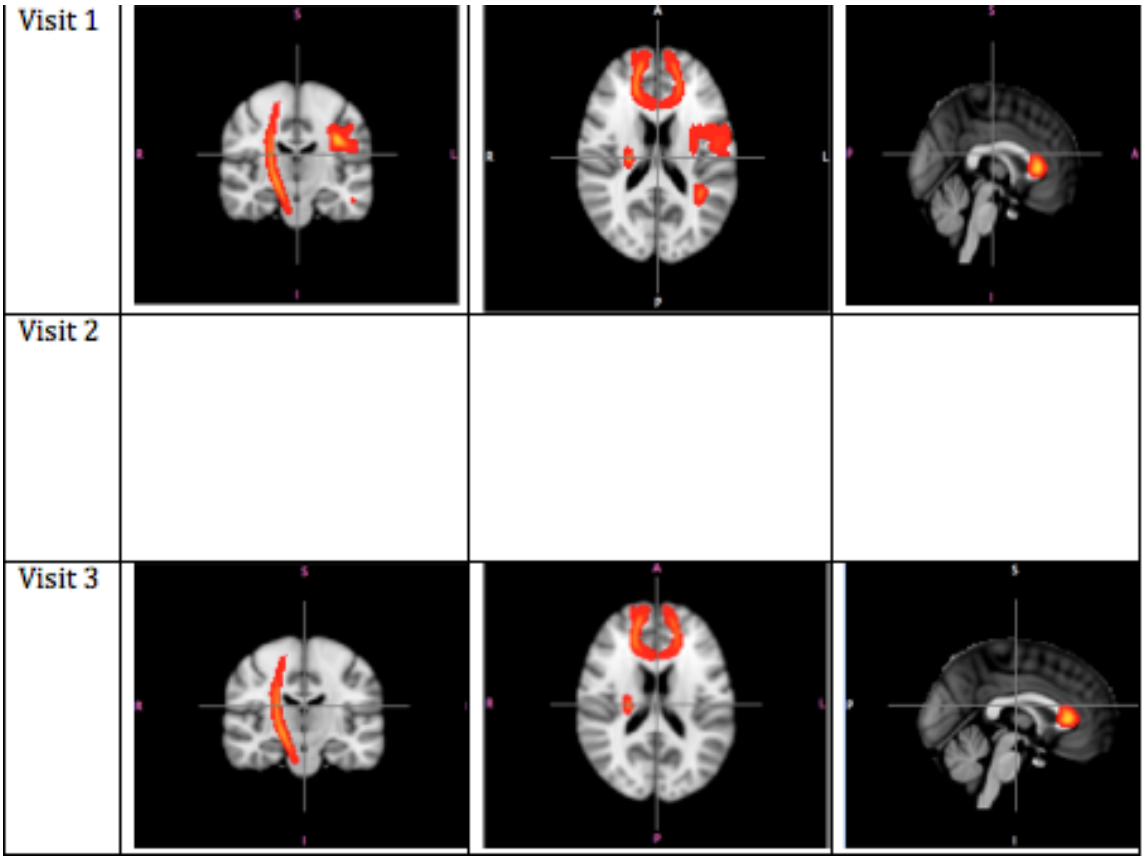

Figure 4.20: FA abnormalities visualizations for all 3 visits

4.2.5 Subject015 (control subject)

- Medical Diagnosis: the patient had an accident and hurt the right front side of his head.

- Graphs:

  – Fractional Anisotropy: From the graph, we can see that there wasnt any significant difference in FA between the patient and the control subject even though there were some minor differences shown.

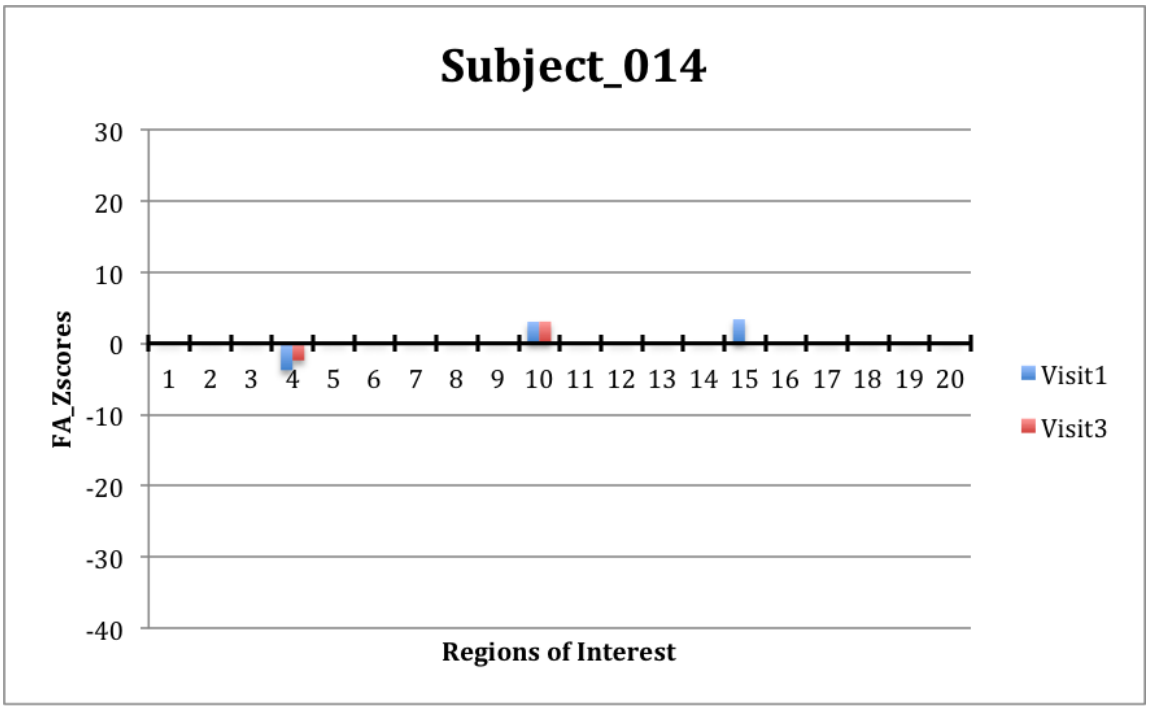

Figure 4.21: FA Z–Scores VS Regions of interest for Subject 014.

– Apparent Diffusion Coefficient: The ADC doesnt show any major statistical difference between the control and the patient. However, the differences here are not negligible.

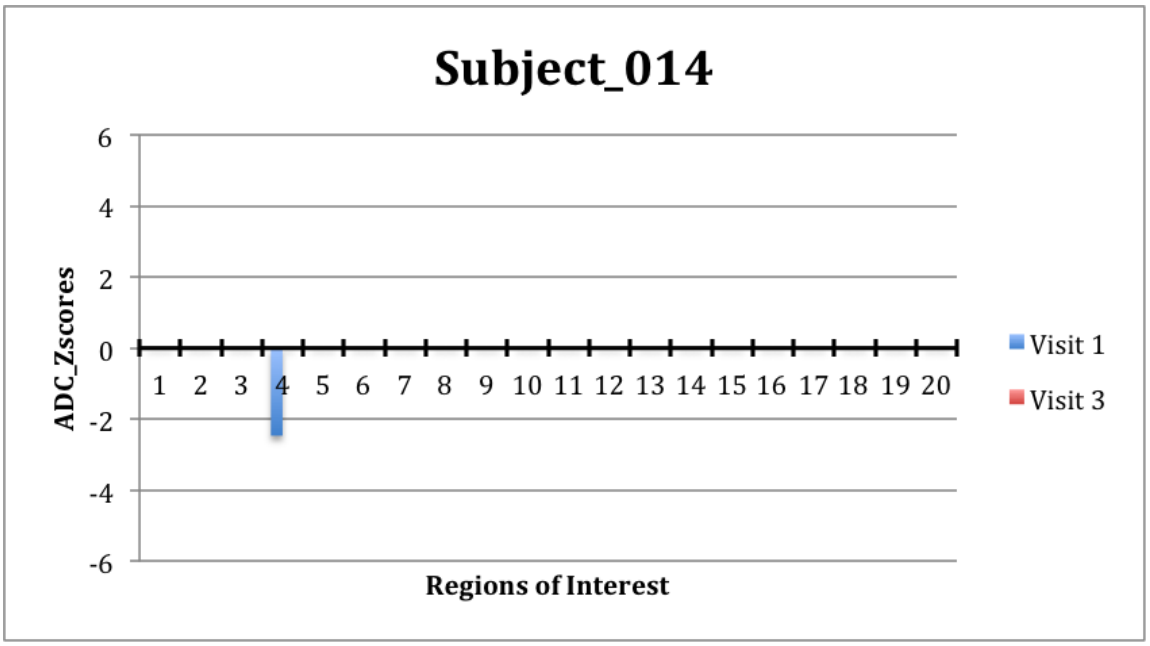

Figure 4.22: ADC Z–Scores VS Regions of interest for Subject 014.

- Visualization: The images below show that the patient was affected on many parts of the brain and it improved on the third visit. This patient did not show up for the second visit.

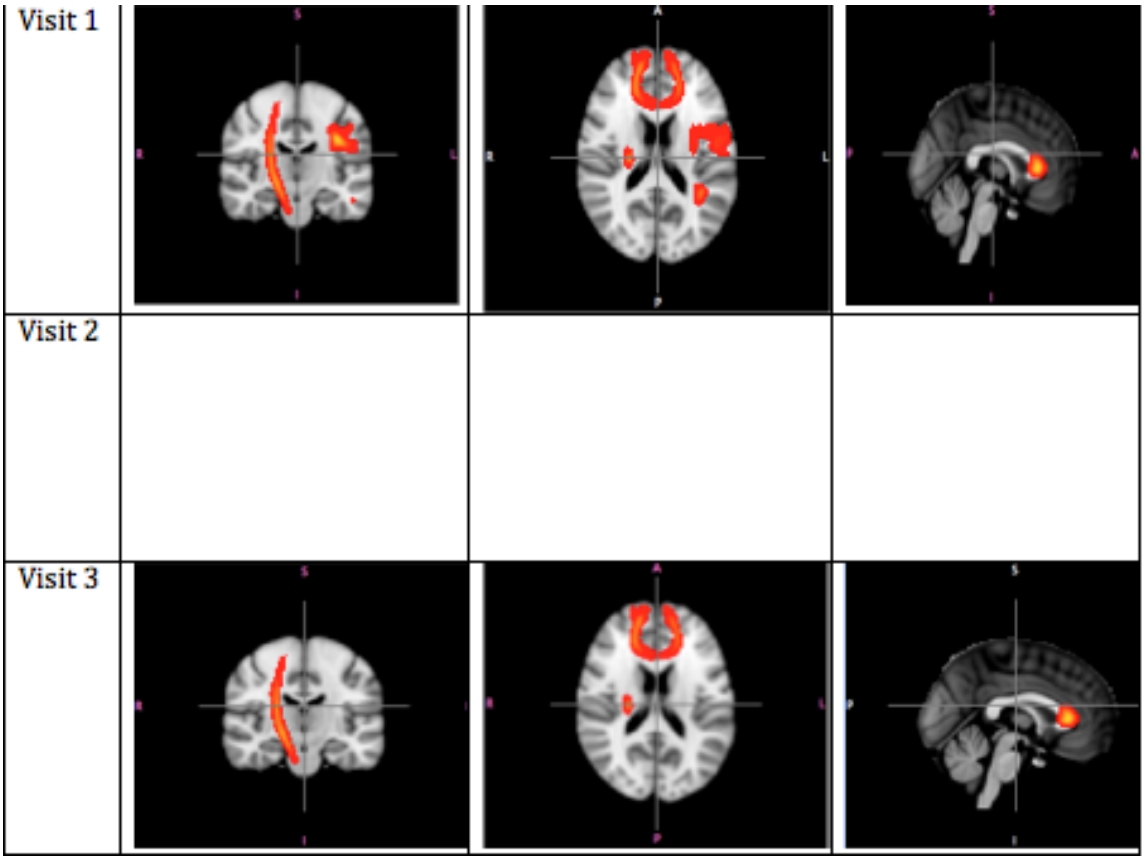

Figure 4.23: FA abnormalities visualizations for all 3 visits

4.2.6 Subject018 (mTBI patient)

- Medical Diagnosis: the patient had a motorcycle accident and hurt the right side of his body.

- Graphs:

  – Fractional Anisotropy: the graph shows that on the first visit, there was a very significant difference in FA in region 15 (Left Superior longitudinal Fasciculus). We can observe improvement in FA in the subsequent visits

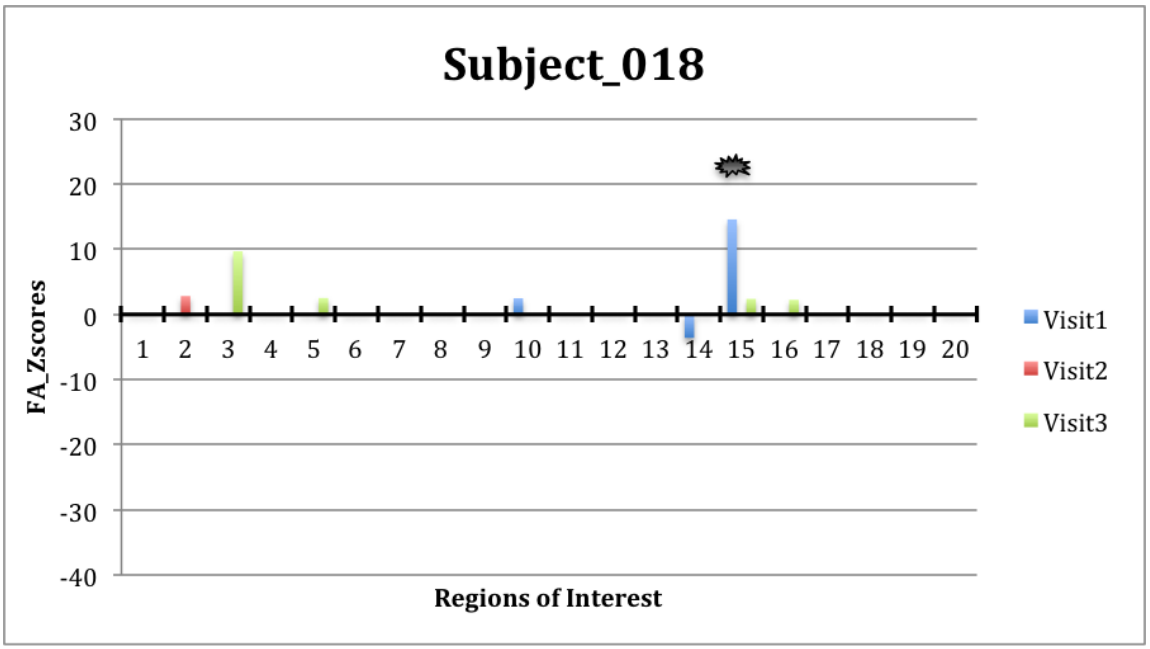

Figure 4.24: FA Z–Scores VS Regions of interest for Subject 018.

– Apparent Diffusion Coefficient: The ADC doesnt show any major statistical difference between the control and the patient. However, the differences here are not negligible.

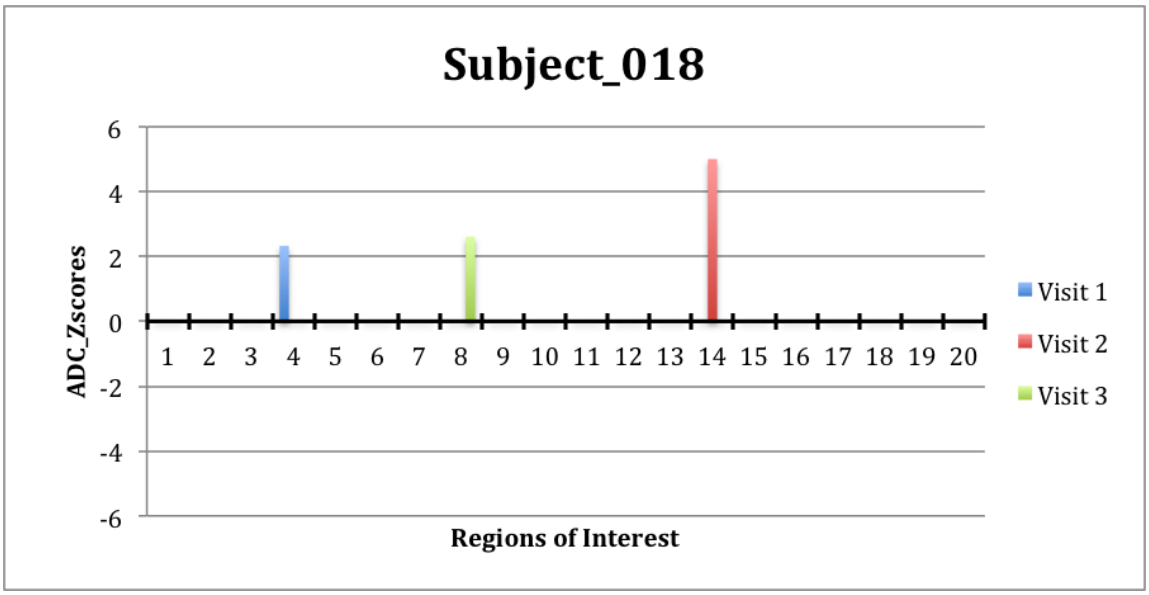

Figure 4.25: ADC Z–Scores VS Regions of interest for Subject 018.

- Visualization: The images below show that the patient was affected on many parts of the brain and it improved during the next visits.

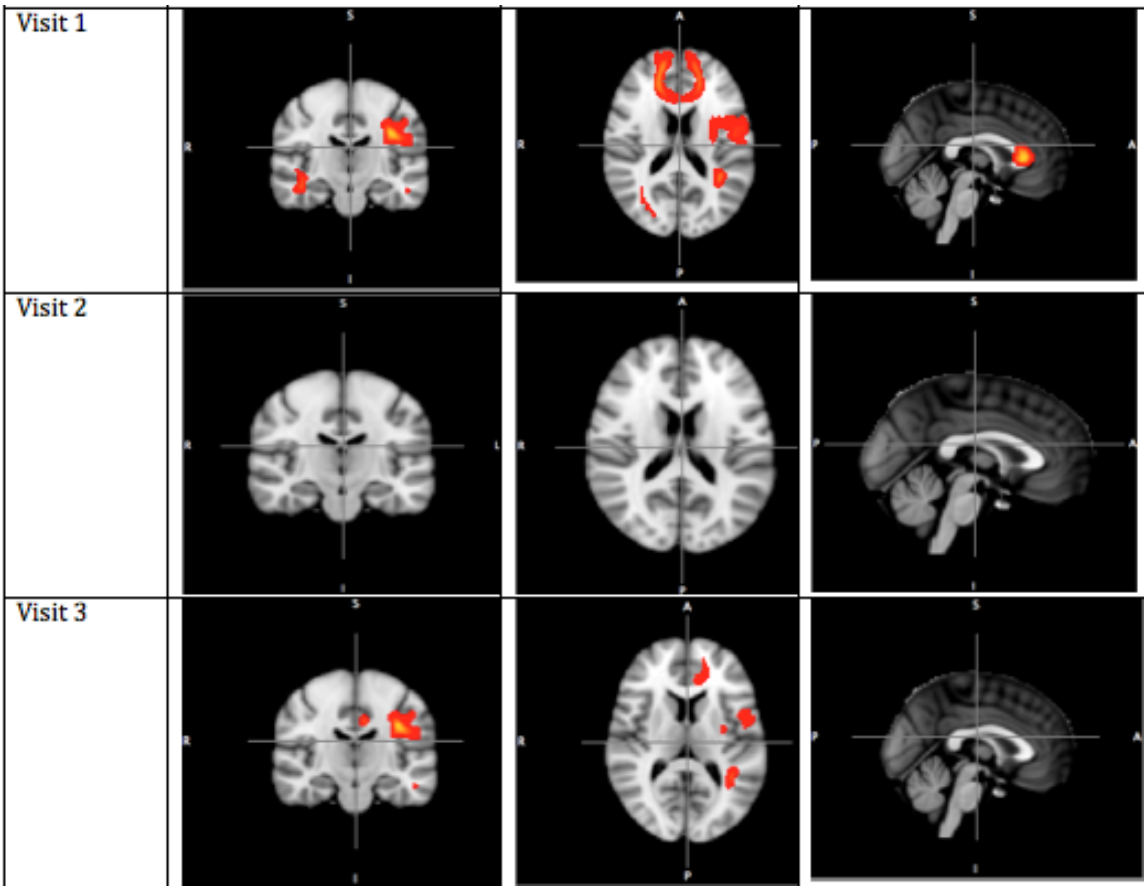

Figure 4.26: FA abnormalities visualizations for all 3 visits

4.2.7 Subject020 (mTBI patient)

- Medical Diagnosis: the patient was hit by a softball and hurt the back side of her head.
- Graphs:
  - Fractional Anisotropy: the graph shows that on the first visit, there was a very significant difference in FA in region 15 (Left Superior longitudinal Fasciculus). We can observe total recovery in the subsequent visits.

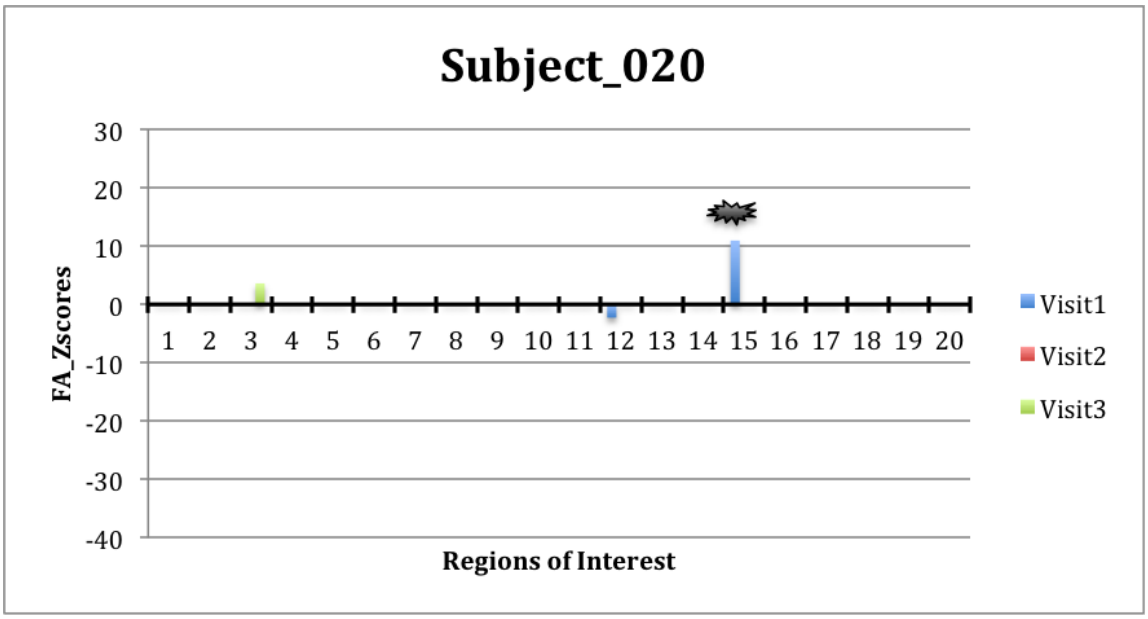

Figure 4.27: FA Z–Scores VS Regions of interest for Subject 020.

– Apparent Diffusion Coefficient: The ADC doesnt show any major statistical difference between the control and the patient. But the differences here are not negligible.

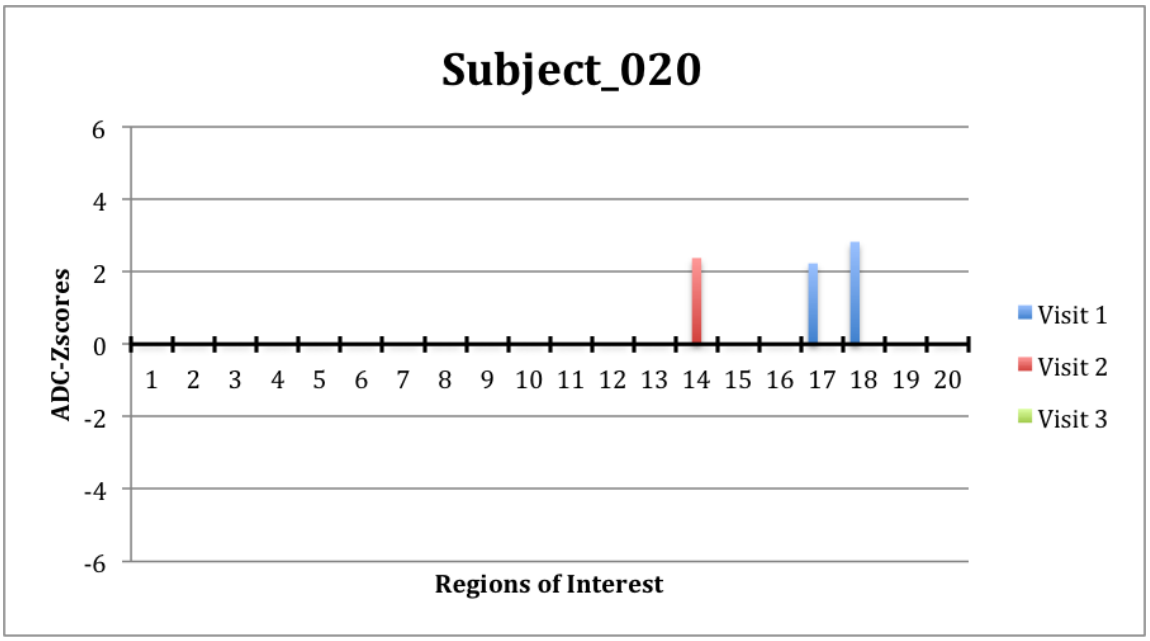

Figure 4.28: ADC Z–Scores VS Regions of interest for Subject 018.

- Visualization: The images below show that the patient was affected on many parts of the brain and we see a complete recovery during the subsequent visits.

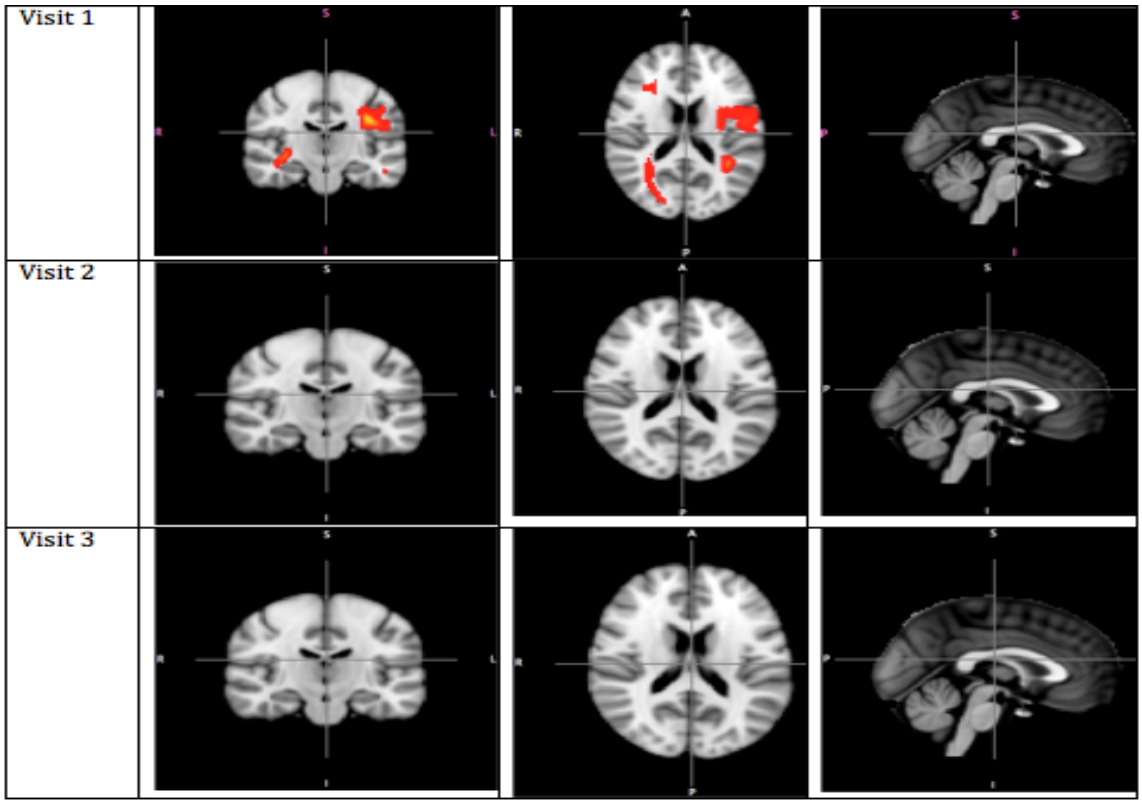

Figure 4.29: FA abnormalities visualizations for all 3 visits

4.2.8 Subject031 (mTBI patient)

- Medical Diagnosis: the patient had a car accident and hit the back of her head .

- Graphs:

  - Fractional Anisotropy: tThe graph shows that there was some minor differences in FA, and we can observe improvements in the subsequent visits.

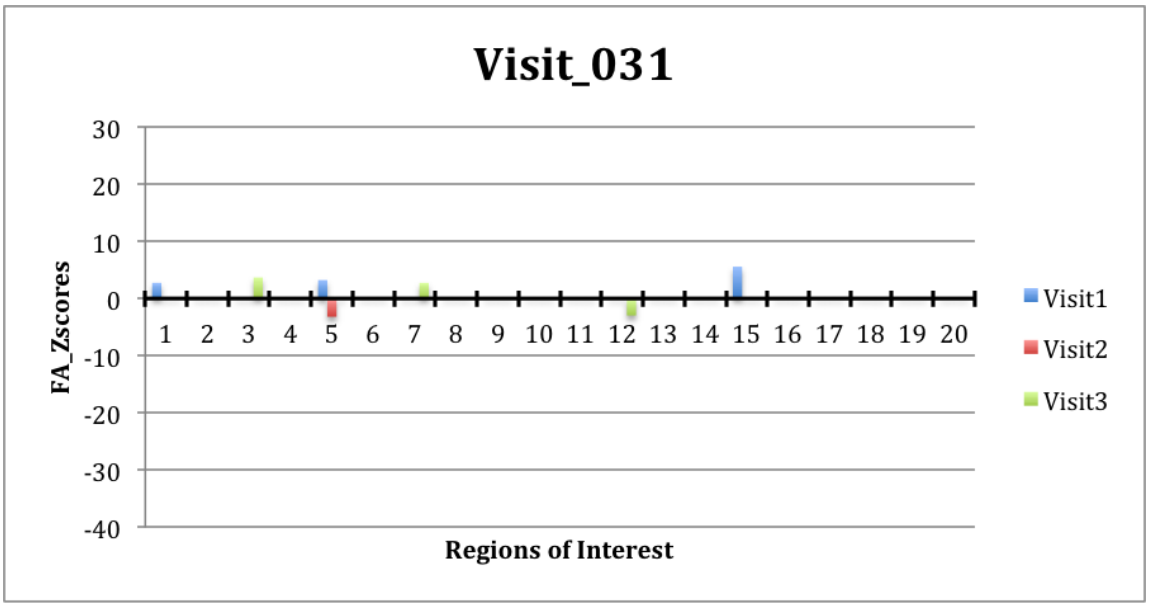

Figure 4.30: FA Z–Scores VS Regions of interest for Subject 031.

– Apparent Diffusion Coefficient: The ADC doesnt show any major statistical difference between the control and the patient. However, the differences here are not negligible.

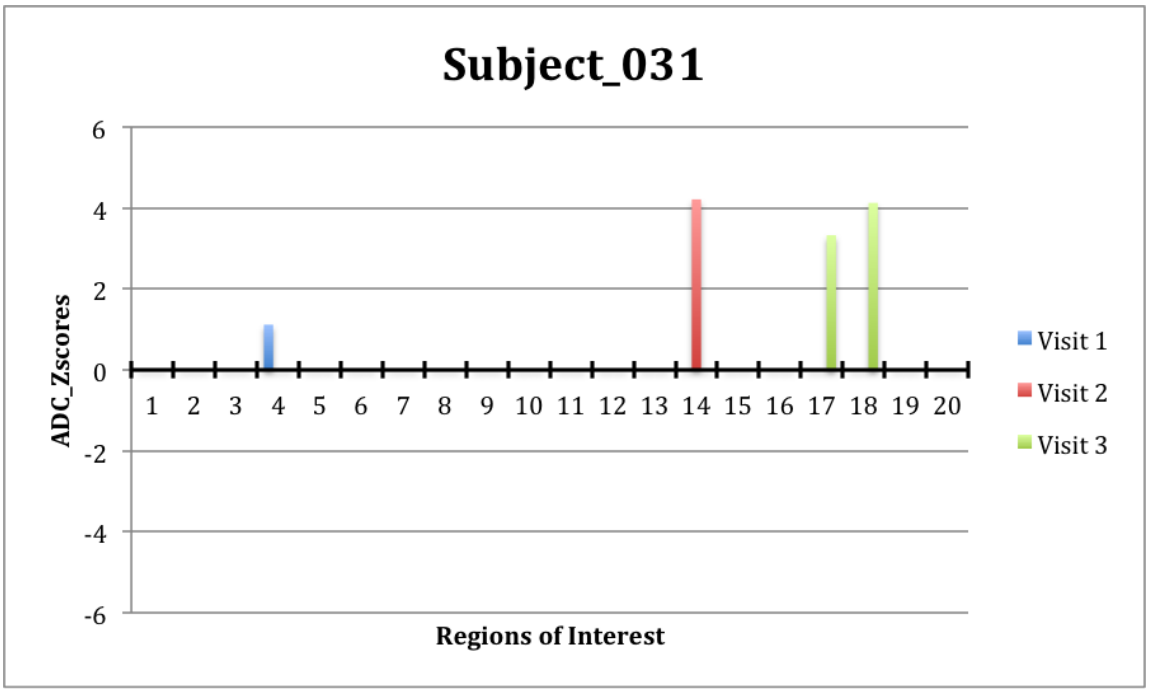

Figure 4.31: ADC Z–Scores VS Regions of interest for Subject 031.

- Visualization: The images below show that the patient was affected on many parts of the brain and it improved during the next visits.

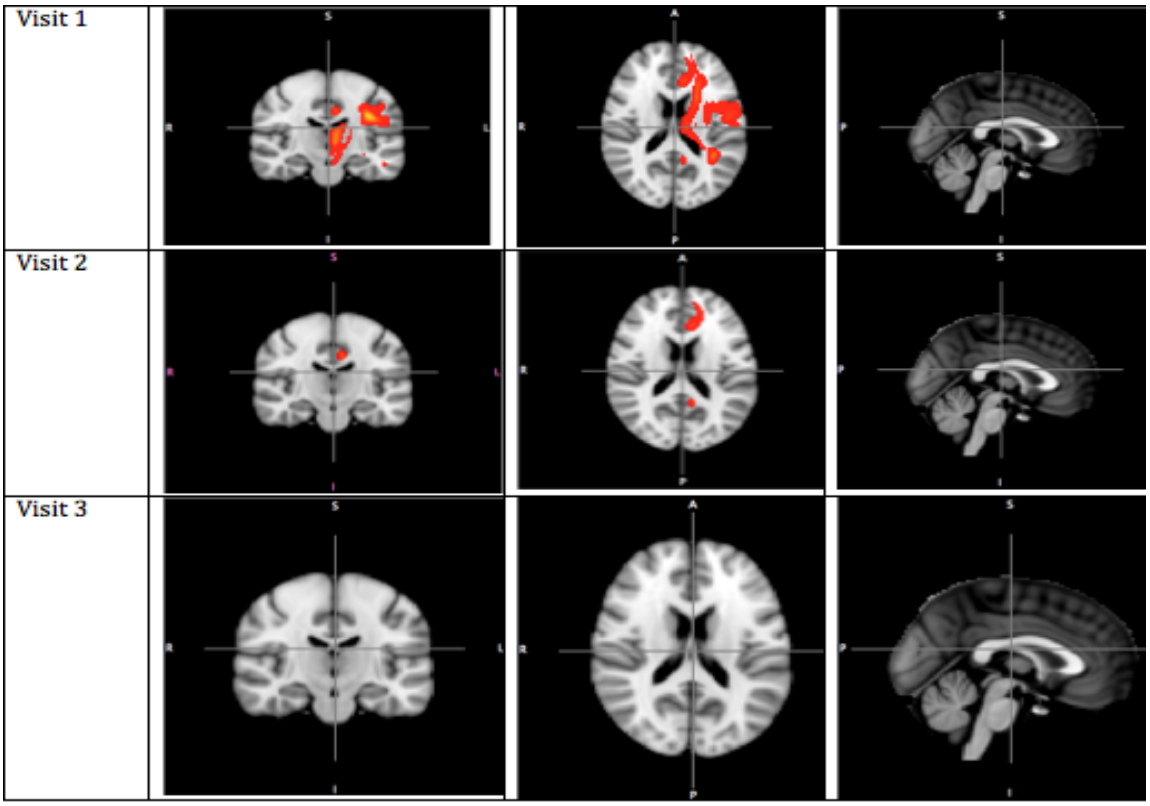

Figure 4.32: FA abnormalities visualizations for all 3 visits

4.2.9 Subject033 (mTBI patient)

- Medical Diagnosis: the patient an accident and hit his head.

- Graphs:

  – Fractional Anisotropy: We see that our patient had a significant difference in FA in region 15 and minor difference in other areas as well. Unfortunately we dont have data for subsequent visits.

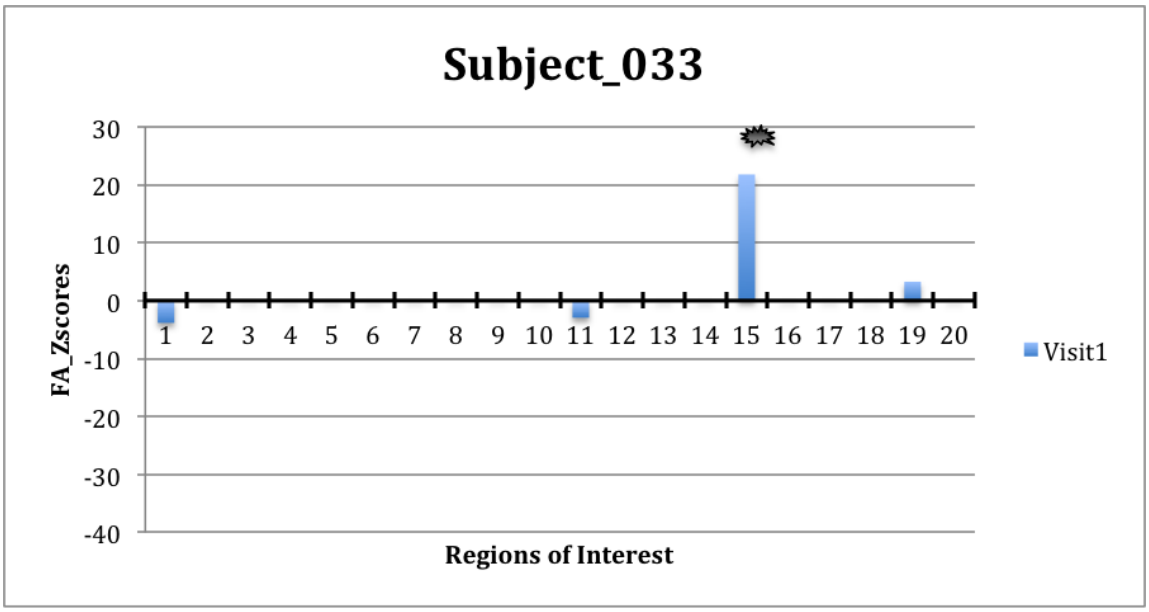

Figure 4.33: FA Z–Scores VS Regions of interest for Subject 033.

– Apparent Diffusion Coefficient: We see that our patient had a significant difference in ADC in region 13 and minor difference in other areas as well. Unfortunately we dont have data for subsequent visits.

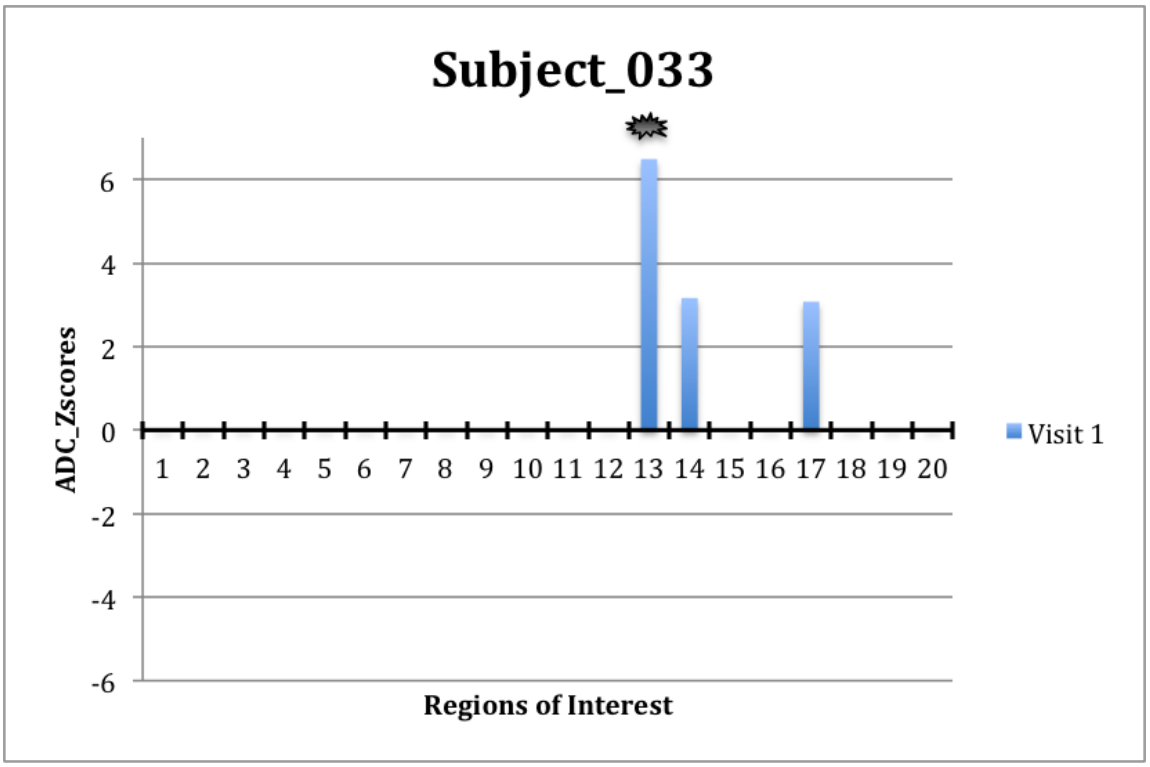

Figure 4.34: ADC Z–Scores VS Regions of interest for Subject 033.

- Visualization: We observe a significant difference in those highlighted parts but unfortunately we dont have data for the next visits.

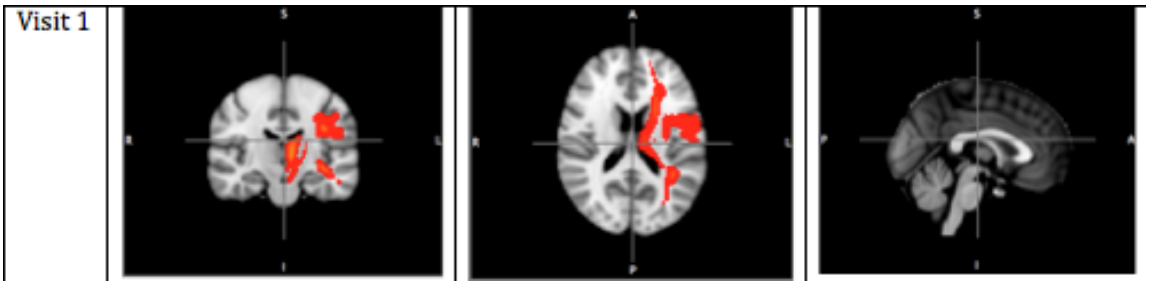

Figure 4.35: FA abnormalities visualizations for all 3 visits

4.2.10 Subject035 (mTBI patient)

- Medical Diagnosis: the patient had a motorcycle accident and hurt the right side of his body.

- Graphs:

  – Fractional Anisotropy: The graph shows that there was some minor differences in FA. We can observe improvement in FA in the subsequent visits

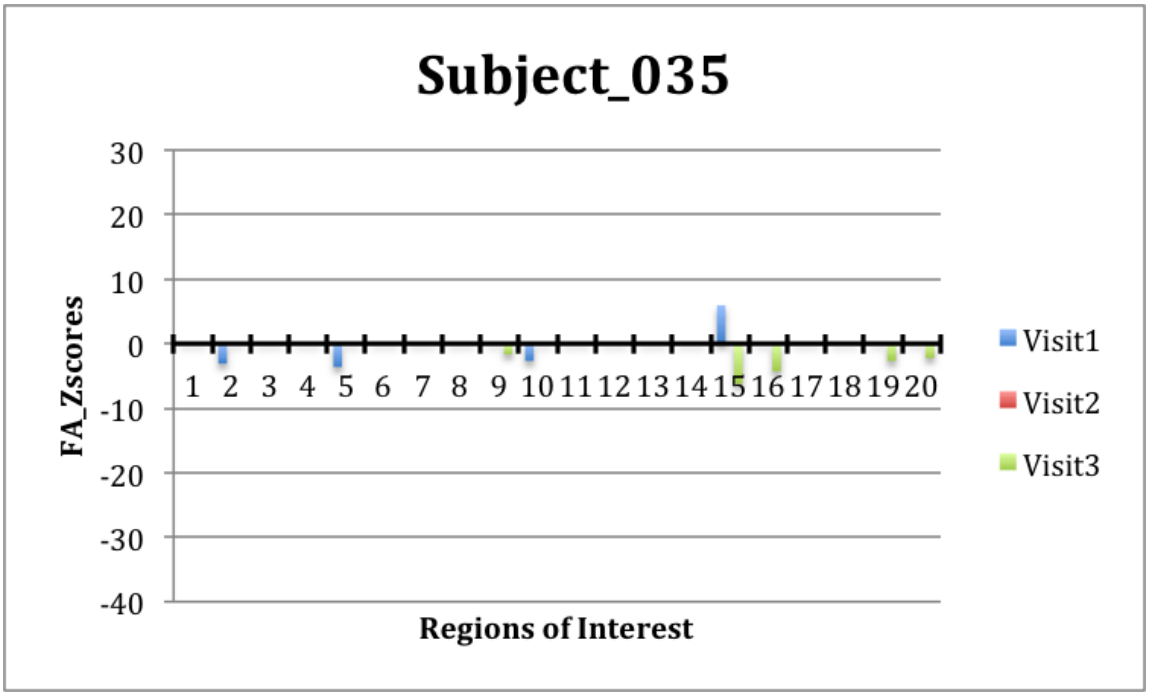

Figure 4.36: FA Z–Scores VS Regions of interest for Subject 035.

  – Apparent Diffusion Coefficient: We see that our patient had a significant difference in ADC in region 17 and minor difference in other areas as well.

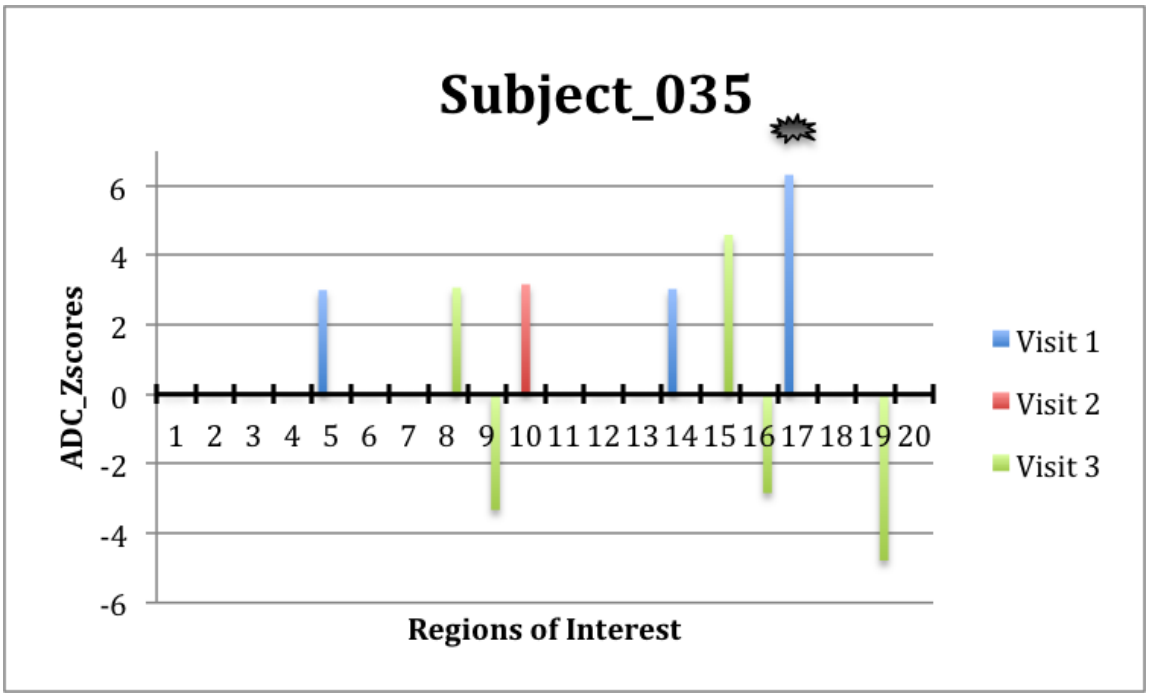

Figure 4.37: ADC Z–Scores VS Regions of interest for Subject 035.

- Visualization: The images below show that the patient was affected on many parts of the brain and it improved during the next visits.

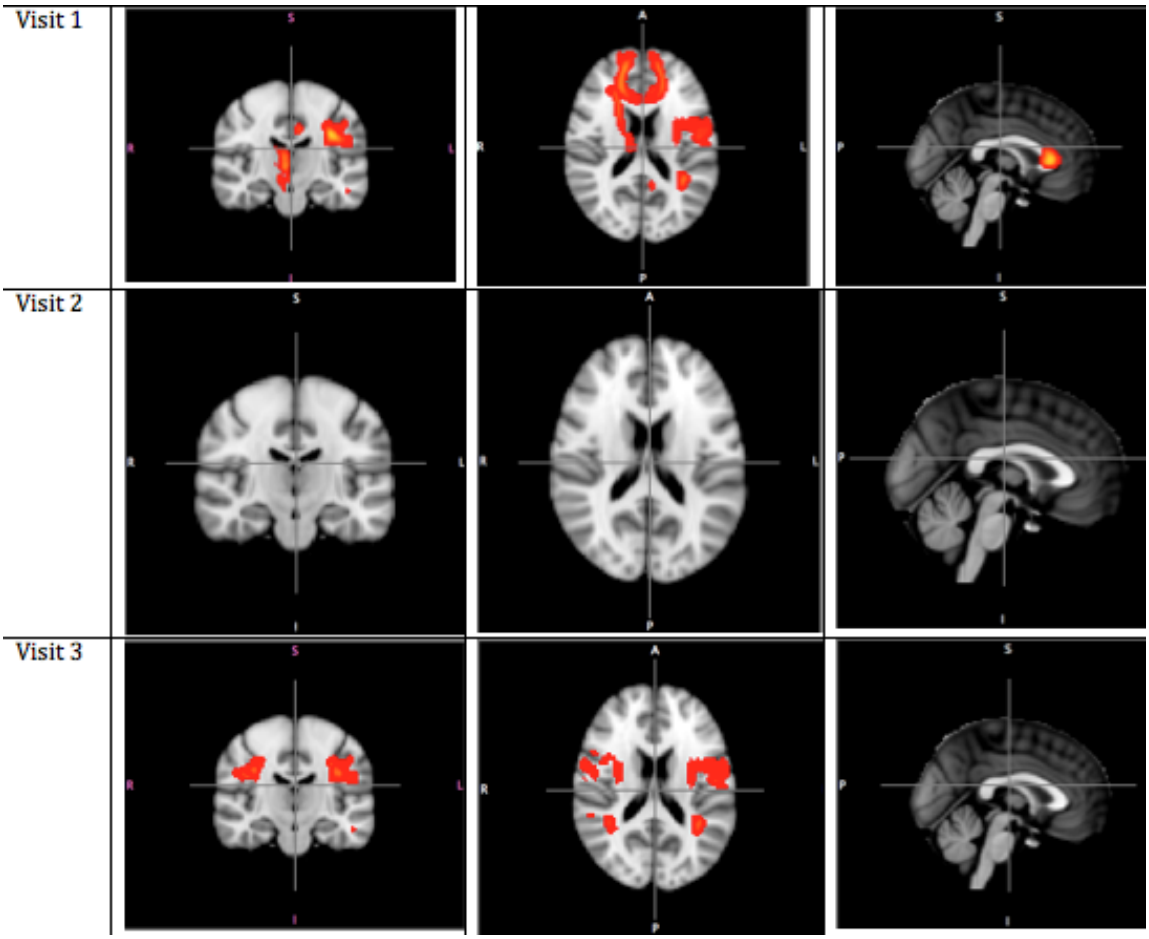

Figure 4.38: FA abnormalities visualizations for all 3 visits

4.2.11 Subject037(mTBI patient)

- Medical Diagnosis: The patient was hit by a 2 ×4 wood on the back right side of the head.

- Graphs:

  – Fractional Anisotropy: We see that our patient had a significant difference

in FA in region 15 and minor difference in other areas as well. Unfortunately we dont have data for subsequent visits.

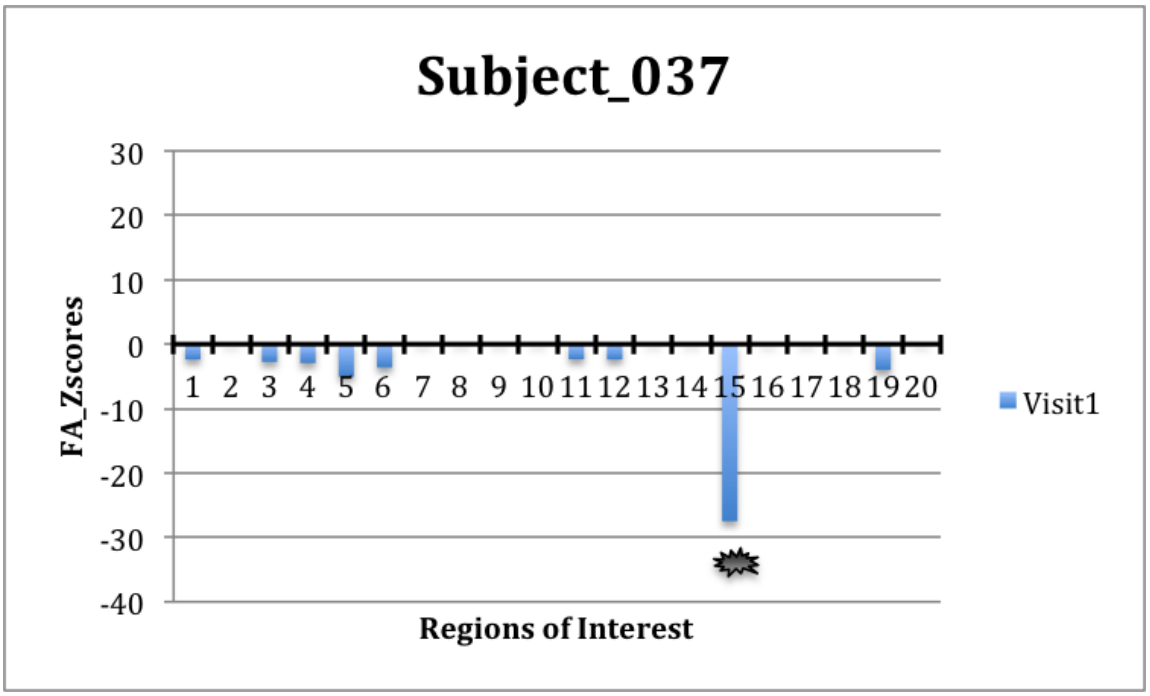

Figure 4.39: FA Z–Scores VS Regions of interest for Subject 037.

– Apparent Diffusion Coefficient: The graph shows the minor differences in the ADC. unfortunately, we don't have data for the next visits.

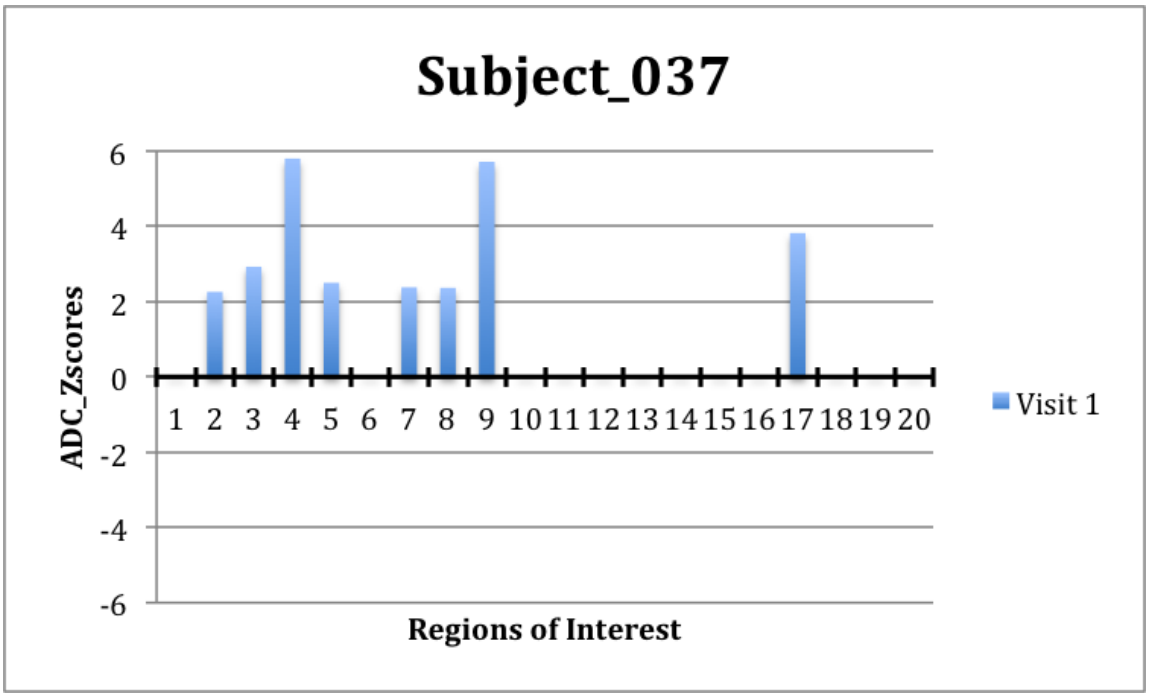

Figure 4.40: ADC Z–Scores VS Regions of interest for Subject 037.

- Visualization: We observe a significant difference in those highlighted parts but unfortunately we dont have data for the next visits.

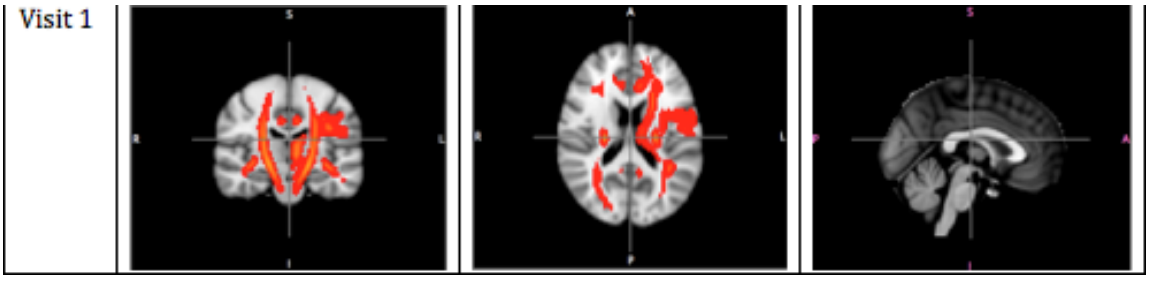

Figure 4.41: FA abnormalities visualizations for all 3 visits

4.2.12 Subject039 (mTBI patient)

- Medical Diagnosis: The patient had a car accident and hurt both temporal parts.

- Graphs:

  – Fractional Anisotropy: We see that our patient had a significant difference in FA in region 15 and minor difference in other areas as well. Unfortunately we dont have data for subsequent visits.

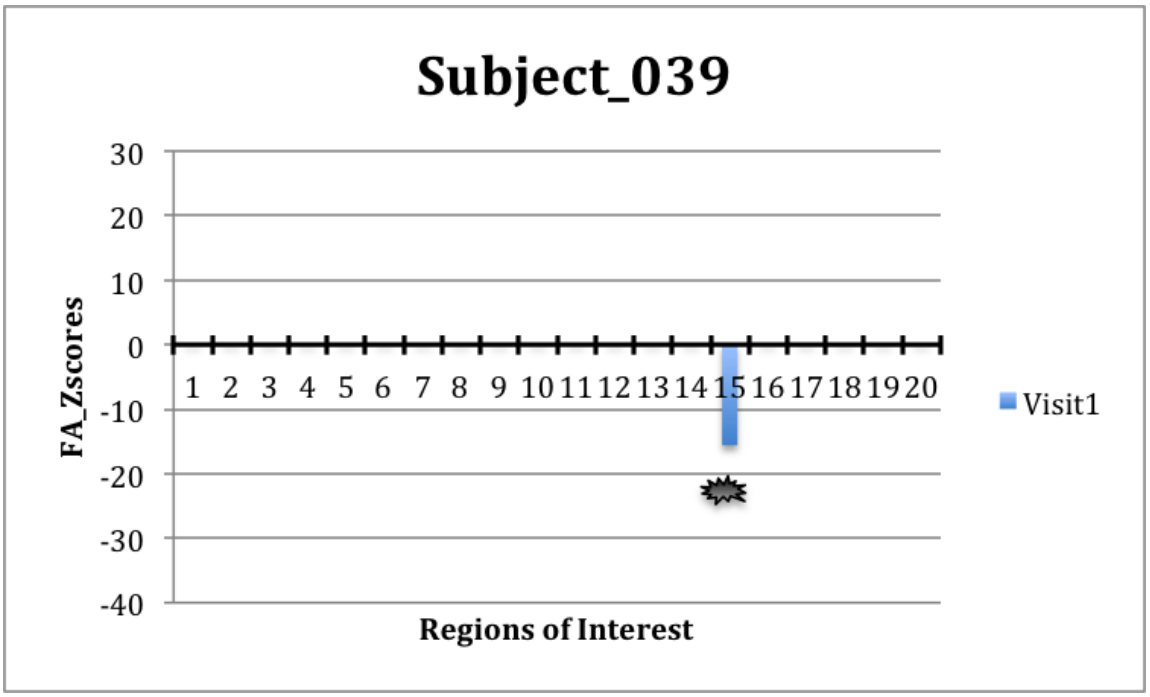

Figure 4.42: FA Z–Scores VS Regions of interest for Subject 039.

  – Apparent Diffusion Coefficient: The graph shows the minor differences in the ADC. unfortunately, we don't have data for the next visits.

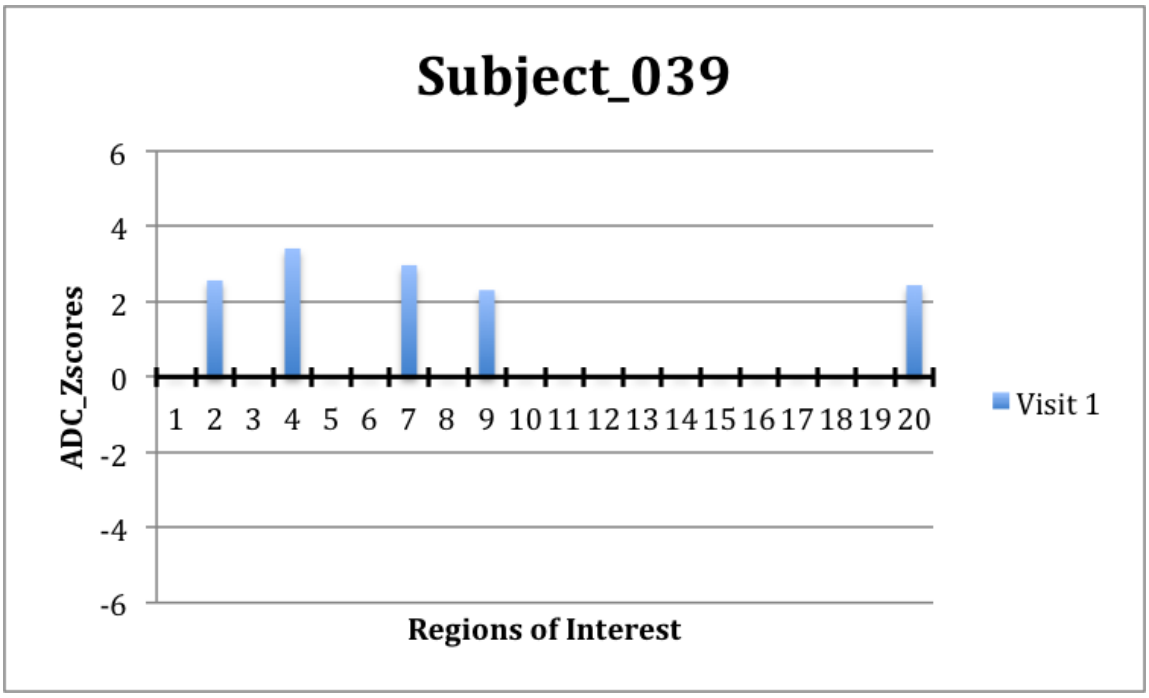

Figure 4.43: ADC Z–Scores VS Regions of interest for Subject 039.

- Visualization: We observe a significant difference in those highlighted parts but unfortunately we dont have data for the next visits.

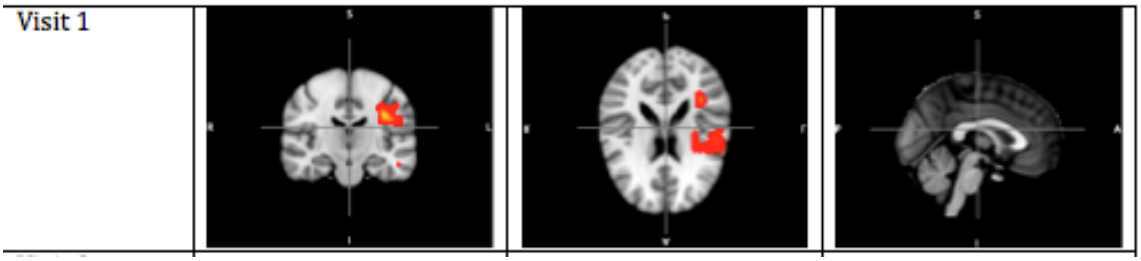

Figure 4.44: FA abnormalities visualizations for all 3 visits

From the statistical results given above, we can see that the two groups were significantly different in FA values, but not in ADC. Furthermore, FA values were significantly different only on the first visit, but not the second or third. The ROIs

with the largest differences were the left and right superior longitudinal fasciculi.

Chapter 5

Conclusion

This chapter is dedicated to the summarization of the results presented in the previous chapter, as well as the conclusions that can be derived from the gathered and collated data. Recommendations for actions as well as further studies are also included in this chapter. As stated in Chapter One, this study aimed at investigating whether DTI could be used to assess recovery in patients with mild traumatic brain injury (mTBI).

5.1 Summary

In summary, we studied how DTI could be an effective technology to detect mTBI, and how we could assess recovery in patients that suffered trauma. We first obtained the diffusion weighed images from a 3.0 T scanner, then we removed noise using FSL, then we acquired quantitative data (FA and ADC) using the software package MedInria; the data was then analyzed by performing a standard z-score for each subjects data and compared the groups using MANOVA with p value set at

0.05, corrected for multiple comparisons, considering group and visit as the independent variables. The results showed us that FA was in fact a sensitive measure to detect injury in mTBI patients, and we saw that the regions of interest with the largest differences were the left and right superior longitudinal fasciculi. These areas, and their four distinct components, are involved with motor behavior and association tasks, perception of visual space, spatial attention, language articulation, and working memory.

5.2 Conclusion

In conclusion, we the results for the quantification of the DTI measures show that FA is a sensitive measure to detect injury in patients with mTBI during the acute phase, and it can also quantify improvement over time that correlate well with clinical measures and subjective patient-reported symptomatology. These findings suggest that FA may be used as a reliable biomarker of mTBI that can help with the diagnosis, prognosis, and assessment of treatment effectiveness. As we said in chapter one, FA can be used to measure white matter integrity; and our e results are consistent with the findings of Cercignani, Mara, *et al.*[44], FA and ADC histograms were different for patients with multiple sclerosis compared with control volunteers. Our first objective of quantifying white matter microstructural changes in mTBI patients was fulfilled. The second objective of this thesis was to assess recovery of the patients, and our results showed that some patients fully recovered, while some only showed an improvement in their condition.

Bibliography

[1] The brain and spinal cord. URL http://www.macmillan.org.uk/information-and-support/brain-tumours/understanding-cancer/the-brain.html.

[2] Brain cell. URL http://vanat.cvm.umn.edu/neurHistAtls/pages/images/Neuron1.gif.

[3] Brain injuries. URL http://www.webmd.com/brain/ss/slideshow-concussions-brain-injuries.

[4] Andrew L Alexander, Jee Eun Lee, Mariana Lazar, and Aaron S Field. Diffusion tensor imaging of the brain. *Neurotherapeutics*, 4(3):316–329, 2007.

[5] Vincent Lai. Application of diffusion–and perfusion–weighted imaging in acute ischemic stroke. *Advanced Brain Neuroimaging Topics in Health and Disease: Methods and Applications*, 2014.

[6] Example of tensor shapes. URL http://www.diffusion-imaging.com/2015/10/what-is-diffusion-tensor.html.

[7] Kegang Hua, Jiangyang Zhang, Setsu Wakana, Hangyi Jiang, Xin Li, Daniel S Reich, Peter A Calabresi, James J Pekar, Peter CM van Zijl, and Susumu Mori.

Tract probability maps in stereotaxic spaces: analyses of white matter anatomy and tract-specific quantification. *Neuroimage*, 39(1):336–347, 2008.

[8] Injury prevention & control: Traumatic brain injury concussion. URL `http://www.cdc.gov/traumaticbraininjury/get`$_t he_f acts.html$.

[9] Thomas Benner, Ruopeng Wang, and J Van Wedeen. Diffusion tensor imaging of the brain. In *Parallel Imaging in Clinical MR Applications*, pages 379–392. Springer, 2007.

[10] ME Shenton, HM Hamoda, JS Schneiderman, S Bouix, O Pasternak, Y Rathi, M-A Vu, MP Purohit, K Helmer, I Koerte, et al. A review of magnetic resonance imaging and diffusion tensor imaging findings in mild traumatic brain injury. *Brain imaging and behavior*, 6(2):137–192, 2012.

[11] Tamer El Sayed, Alejandro Mota, Fernando Fraternali, and Michael Ortiz. Biomechanics of traumatic brain injury. *Computer Methods in Applied Mechanics and Engineering*, 197(51):4692–4701, 2008.

[12] Jeffrey T Barth, Jason R Freeman, Donna K Broshek, and Robert N Varney. Acceleration-deceleration sport-related concussion: the gravity of it all. *Journal of Athletic Training*, 36(3):253, 2001.

[13] WL Maxwell, C Watt, DI Graham, and TA Gennarelli. Ultrastructural evidence of axonal shearing as a result of lateral acceleration of the head in non-human primates. *Acta neuropathologica*, 86(2):136–144, 1993.

[14] Takeshi Imajo and Uros Roessman. Diffuse axonal injury. *The American journal of forensic medicine and pathology*, 5(3):217–222, 1984.

[15] Stavros I Dimitriadis, George Zouridakis, Roozbeh Rezaie, Abbas Babajani-Feremi, and Andrew C Papanicolaou. Functional connectivity changes detected with magnetoencephalography after mild traumatic brain injury. *NeuroImage: Clinical*, 9:519–531, 2015.

[16] Marios Antonakakis, Stavros I Dimitriadis, Michalis Zervakis, Sifis Micheloyannis, Roozbeh Rezaie, Abbas Babajani-Feremi, George Zouridakis, and Andrew C Papanicolaou. Altered cross-frequency coupling in resting-state meg after mild traumatic brain injury. *International Journal of Psychophysiology*, 102:1–11, 2016.

[17] Edith V Sullivan and Adolf Pfefferbaum. Diffusion tensor imaging and aging. *Neuroscience & Biobehavioral Reviews*, 30(6):749–761, 2006.

[18] Peter J Basser, James Mattiello, and Denis LeBihan. Mr diffusion tensor spectroscopy and imaging. *Biophysical journal*, 66(1):259, 1994.

[19] Denis Le Bihan, Jean-François Mangin, Cyril Poupon, Chris A Clark, Sabina Pappata, Nicolas Molko, and Hughes Chabriat. Diffusion tensor imaging: concepts and applications. *Journal of magnetic resonance imaging*, 13(4):534–546, 2001.

[20] Phyllis I Edwards. Robert brown (1773-1858) and the natural history of matthew flinders' voyage in hms investigator, 1801-1805. *Journal of the Society for the Bibliography of Natural History*, 7(4):385–407, 1976.

[21] Albert Einstein. *Investigations on the Theory of the Brownian Movement*. Courier Corporation, 1956.

[22] Brain cell. URL `http://spinwarp.ucsd.edu/NeuroWeb/Text/br-710dwi.htm`.

[23] Jose Soares, Paulo Marques, Victor Alves, and Nuno Sousa. A hitchhiker's guide to diffusion tensor imaging. *Frontiers in neuroscience*, 7:31, 2013.

[24] PC Sundgren, Q Dong, D Gomez-Hassan, SK Mukherji, P Maly, and R Welsh. Diffusion tensor imaging of the brain: review of clinical applications. *Neuroradiology*, 46(5):339–350, 2004.

[25] J Head. Definition of mild traumatic brain.. injury. *J Head Trauma Rehabil*, 8 (3):86–87, 1993.

[26] F Gerstenbrand and Ch A Stepan. Mild traumatic brain injury. *Brain Injury*, 15(2):95–97, 2001.

[27] Denis Le Bihan and E Breton. Imagerie de diffusion in-vivo par résonance magnétique nucléaire. *Comptes-Rendus de l'Académie des Sciences*, 93(5):27–34, 1985.

[28] Edward O Stejskal and John E Tanner. Spin diffusion measurements: spin echoes in the presence of a time-dependent field gradient. *The journal of chemical physics*, 42(1):288–292, 1965.

[29] GG Cleveland, DC Chang, CF Hazlewood, and HE Rorschach. Nuclear magnetic resonance measurement of skeletal muscle: anisotrophy of the diffusion coefficient of the intracellular water. *Biophysical journal*, 16(9):1043, 1976.

[30] Thomas L Chenevert, James A Brunberg, and James G Pipe. Anisotropic diffusion in human white matter: demonstration with mr techniques in vivo. *Radiology*, 177(2):401–405, 1990.

[31] Mark Doran, Joseph V Hajnal, Nicholas Van Bruggen, Martin D King, Ian R Young, and Graeme M Bydder. Normal and abnormal white matter tracts shown by mr imaging using directional diffusion weighted sequences. *Journal of computer assisted tomography*, 14(6):865–873, 1990.

[32] Derek K Jones and Alexander Leemans. Diffusion tensor imaging. *Magnetic Resonance Neuroimaging: Methods and Protocols*, pages 127–144, 2011.

[33] Matilde Inglese, Sachin Makani, Glyn Johnson, Benjamin A Cohen, Jonathan A Silver, Oded Gonen, and Robert I Grossman. Diffuse axonal injury in mild traumatic brain injury: a diffusion tensor imaging study. *Journal of neurosurgery*, 103(2):298–303, 2005.

[34] Jeffrey J Bazarian, Jianhui Zhong, Brian Blyth, Tong Zhu, Voyko Kavcic, and Derick Peterson. Diffusion tensor imaging detects clinically important axonal damage after mild traumatic brain injury: a pilot study. *Journal of neurotrauma*, 24(9):1447–1459, 2007.

[35] EA Wilde, SR McCauley, JV Hunter, ED Bigler, Z Chu, ZJ Wang, GR Hanten, M Troyanskaya, R Yallampalli, X Li, et al. Diffusion tensor imaging of acute mild traumatic brain injury in adolescents. *Neurology*, 70(12):948–955, 2008.

[36] DR Rutgers, F Toulgoat, J Cazejust, P Fillard, P Lasjaunias, and D Ducreux.

White matter abnormalities in mild traumatic brain injury: a diffusion tensor imaging study. *American Journal of Neuroradiology*, 29(3):514–519, 2008.

[37] Diffusion tensor imaging tutorial. URL `http://www.diffusion-imaging.com/2015/10/dti-tutorial-1-from-scanner-to-tensor.html`.

[38] Chloe Hutton, Andreas Bork, Oliver Josephs, Ralf Deichmann, John Ashburner, and Robert Turner. Image distortion correction in fmri: a quantitative evaluation. *Neuroimage*, 16(1):217–240, 2002.

[39] C Rorden, HO Karnath, and L Bonilha. Mricron dicom to nifti converter. *Neuroimaging Informatics Tools and Resources Clearinghouse (NITRC). Available from: http://www. mccauslandcenter. sc. edu/mricro/mricron/dcm2nii. html, Accessed on June*, 7, 2012.

[40] Jesper LR Andersson, Stefan Skare, and John Ashburner. How to correct susceptibility distortions in spin-echo echo-planar images: application to diffusion tensor imaging. *Neuroimage*, 20(2):870–888, 2003.

[41] Mark W Woolrich, Saad Jbabdi, Brian Patenaude, Michael Chappell, Salima Makni, Timothy Behrens, Christian Beckmann, Mark Jenkinson, and Stephen M Smith. Bayesian analysis of neuroimaging data in fsl. *Neuroimage*, 45(1):S173–S186, 2009.

[42] Nicolas Toussaint, Jean-Christophe Souplet, Pierre Fillard, et al. Medinria: medical image navigation and research tool by inria. In *Proc. of MICCAI*, volume 7, page 280. Citeseer, 2007.

[43] SAS Institute. *SAS/STAT user's guide: Version 6*, volume 2. Sas Inst, 1990.

[44] Mara Cercignani, Matilde Inglese, Elisabetta Pagani, Giancarlo Comi, and Massimo Filippi. Mean diffusivity and fractional anisotropy histograms of patients with multiple sclerosis. *American Journal of Neuroradiology*, 22(5):952–958, 2001.